

Homophily Heterogeneity Matters in Graph Federated Learning: A Spectrum Sharing and Complementing Perspective

Wentao Yu, *Student Member, IEEE*

Abstract—Since heterogeneity presents a fundamental challenge in graph federated learning, many existing methods are proposed to deal with node feature heterogeneity and structure heterogeneity. However, they overlook the critical homophily heterogeneity, which refers to the substantial variation in homophily levels across graph data from different clients. The homophily level represents the proportion of edges connecting nodes that belong to the same class. Due to adapting to their local homophily, local models capture inconsistent spectral properties across different clients, significantly reducing the effectiveness of collaboration. Specifically, local models trained on graphs with high homophily tend to capture low-frequency information, whereas local models trained on graphs with low homophily tend to capture high-frequency information. To effectively deal with homophily heterogeneity, we introduce the spectral Graph Neural Network (GNN) and propose a novel Federated learning method by mining Graph Spectral Properties (FedGSP). On one hand, our proposed FedGSP enables clients to share generic spectral properties (*i.e.*, low-frequency information), allowing all clients to benefit through collaboration. On the other hand, inspired by our theoretical findings, our proposed FedGSP allows clients to complement non-generic spectral properties by acquiring the spectral properties they lack (*i.e.*, high-frequency information), thereby obtaining additional information gain. Extensive experiments conducted on six homophilic and five heterophilic graph datasets, across both non-overlapping and overlapping settings, validate the superiority of our method over eleven state-of-the-art methods. Notably, our FedGSP outperforms the second-best method by an average margin of 3.28% on all heterophilic datasets.

Index Terms—Graph federated learning, Personalized federated learning, Spectral graph neural network.

I. INTRODUCTION

Graph is a type of fundamental data structure across various domains, including social networks, transportation systems, and molecular chemistry [1]–[5]. In real-world applications, large-scale graphs are often partitioned into lots of subgraphs and distributed across multiple clients. However, these distributed subgraphs cannot be combined together to train a centralized model, which is restricted by privacy regulations and data protection protocols. Graph Federated Learning (GFL) [6]–[9] has emerged as a promising approach for collaboratively training models on distributed subgraphs while preserving data privacy.

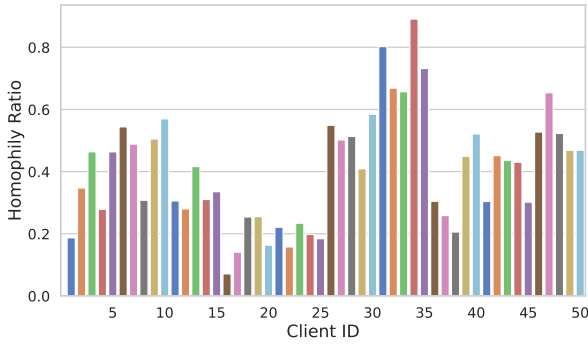
However, the distributions of subgraphs on different clients are inconsistent, leading to heterogeneity and significantly reducing the effectiveness of federated collaboration [10]–[12]. To deal with the heterogeneity issue, lots of GFL methods have been proposed. For example, FedGTA [13] employs a

topology-aware optimization method to solve the structure heterogeneity in GFL. Meanwhile, FED-PUB [6] solves the node feature heterogeneity. Specifically, FED-PUB utilizes the node embeddings of local models to compute the similarities among clients and then performs the weighted averaging of local model parameters. In contrast, FGSSL [7] and Fed-TAD [8] deal with the node feature heterogeneity and structure heterogeneity, simultaneously.

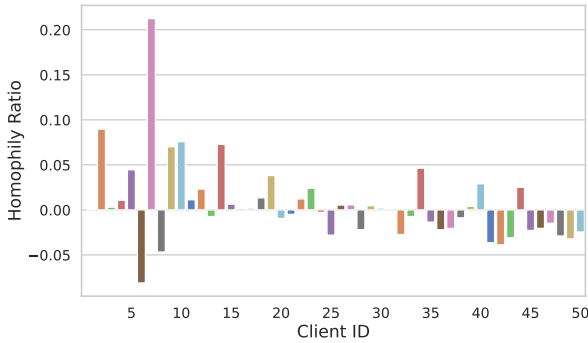
Despite the above-mentioned methods exploring the node feature heterogeneity and structure heterogeneity, they fail to consider the critical homophily heterogeneity. The homophily heterogeneity refers to the significant differences in homophily levels exhibited by graph data across different clients. Homophily refers to the property that edges tend to connect similar nodes [14]. For example, people in social networks tend to connect to others with similar hobbies. To measure the level of homophily, we employ the *adjusted homophily* [14], which solves the issues that existing measures (*e.g.*, edge homophily [15]) are sensitive to the number of classes and their balance (see Appendix VI). Generally, the higher the homophily level, the stronger the homophily. As shown in Fig. 1a, client 34 has graph data with the highest homophily level (*i.e.*, 0.891), while client 16 has graph data with the lowest homophily level (*i.e.*, 0.071). Similarly, as shown in Fig. 1b, client 7 has graph data with the highest homophily level (*i.e.*, 0.212), while client 6 has graph data with the lowest homophily level (*i.e.*, -0.081). Since local models on clients adapt to their corresponding homophily levels [16]–[19], local models capture inconsistent spectral properties across different clients. Specifically, local models trained on graphs with high homophily tend to capture low-frequency information (see Fig. 2a and Fig. 2c), whereas local models trained on graphs with low homophily tend to capture high-frequency information (see Fig. 2b and Fig. 2d). Inconsistent spectral properties captured by different clients pose the challenge to federated aggregation, leading to sub-optimal collaborative effectiveness. Therefore, we raise the following research question:

Since homophily heterogeneity matters in graph federated learning, how can we deal with it?

To answer this question and deal with the homophily heterogeneity issue, we aim to introduce the spectral Graph Neural Network (GNN) as the local model and further theoretically analyze the heterogeneity in GFL. Since spectral GNNs are made up of polynomial bases, they can be easily split into low-frequency and high-frequency parts for subsequent analysis.



(a) Subgraphs partitioned from *CiteSeer* dataset

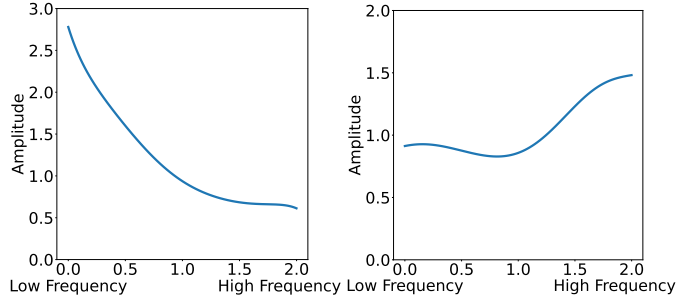


(b) Subgraphs partitioned from *Questions* dataset

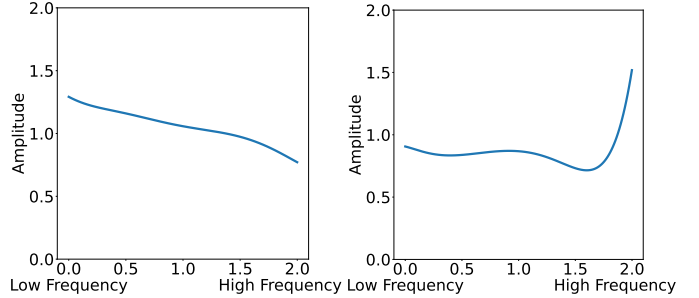
Fig. 1. Homophily levels across clients vary significantly in subgraphs from the *CiteSeer* and *Questions* datasets.

Moreover, we propose a novel **F**ederated learning method by mining **G**raph **S**pectral **P**roperties (FedGSP). Specifically, on one hand, since low-frequency information contains generic spectral properties [20], [21], we enable clients to share generic spectral properties (*i.e.*, low-frequency information), thus allowing all clients to benefit through collaboration. Meanwhile, we theoretically find that the heterogeneity in GFL is proportional to the complementarity ratio. Our theoretical findings inspires us that to deal with the heterogeneity in GFL, we should pursue not only similarities between different clients but also complementarities between different clients. Therefore, on the other hand, we allow clients to complement non-generic spectral properties by acquiring the spectral properties they lack (*i.e.*, high-frequency information), thereby obtaining additional information gain [22], [23]. These strategies allow the local model on each client not only to preserve its local graph spectral properties, but also to benefit from collaborations.

Moreover, since we introduce the spectral GNN as the local model, we propose a novel federated aggregation method from the perspective of polynomial bases, which are fundamental components in the spectral GNNs. By doing so, our proposed FedGSP not only effectively alleviates the homophily heterogeneity, but also significantly improves the model performances on graphs with different homophily levels. Notably, we compare our proposed FedGSP with eleven state-of-the-art methods on six homophilic and five heterophilic graph



(a) Client 34 of *CiteSeer* dataset (homophily level=0.891) (b) Client 16 of *CiteSeer* dataset (homophily level=0.071)



(c) Client 7 of *Questions* dataset (homophily level=0.212) (d) Client 6 of *Questions* dataset (homophily level=-0.081)

Fig. 2. Spectral properties captured by local models vary across clients: (a) and (c) emphasize low-frequency information; (b) and (d) highlight high-frequency information.

datasets, and the experimental results validate the effectiveness of our proposed FedGSP. The key contributions of our work are as follows:

- This is the *first* work to deal with the homophily heterogeneity in GFL, which leads to inconsistent spectral properties across different clients. Therefore, we introduce the spectral GNN as the local model, so that we can mine graph spectral properties for GFL.
- We are the *first* to prove that the heterogeneity in GFL is proportional to the complementarity ratio. Inspired by our theoretical findings, we propose a novel FedGSP method. It not only shares generic spectral properties but also complements non-generic spectral properties among different clients, so that we can successfully alleviate the homophily heterogeneity and improve the effectiveness of GFL.
- Extensive experiments on eleven datasets demonstrate the superiority of our proposed FedGSP over eleven state-of-the-art methods, where our FedGSP outperforms the second-best method by an average margin of 3.28% on all heterophilic datasets. Moreover, case studies validate that our proposed FedGSP allows the local model on each client not only to preserve its local graph spectral properties, but also to obtain the additional spectral properties from collaborations.

II. RELATED WORK

In this section, we review the typical work related to this paper, including GFL, PFL, and Spectral GNNs.

A. Graph Federated Learning

GFL aims to utilize the distributed learning framework to collaboratively train GNNs while maintaining the privacy and security of the local graphs. Most of the existing GFL methods can be categorized into two types: optimization-based methods and model-based methods. On one hand, optimization-based methods focus on optimizing the collaboration strengths between clients, often leveraging conventional GNNs (e.g., Graph Convolutional Networks (GCN) [24]). For instance, FED-PUB [6] determines client collaboration strengths according to the estimated similarities between subgraphs based on the outputs of local GCN-based models. Similarly, FedGTA [13] introduces the optimization-driven federated learning algorithm that adjusts the weight of each client's contribution based on the mixed moments of processed neighbor features. On the other hand, model-based methods focus on designing specific local models while using simple federation strategies (e.g., FedAvg [25]). For example, FedSage+ [26] builds on FedSage [26] by introducing a missing neighbor generator to address missing links across local subgraphs, while FedSage itself combines GraphSAGE [27] with FedAvg. To deal with the structure heterogeneity, AdaFGL [28] introduces homophilous and heterophilous propagation modules for each client so that each client's model is adapted to the local graph structures. Besides, FedTAD [8] enhances the knowledge transfer from the local models to the global model, alleviating the negative impact of unreliable knowledge caused by node feature heterogeneity. However, both optimization-based methods and model-based methods have performance limitations because they overlook the critical homophily heterogeneity, which leads to inconsistent spectral properties across different clients. Therefore, we naturally introduce the spectral GNN as the local model to mine graph spectral properties for GFL.

B. Personalized Federated Learning

Heterogeneity presents a fundamental challenge in GFL [29]. To deal with the heterogeneity, PFL methods [30]–[32] have obtained increasing attention. Unlike FedAvg, which aims to train a global model collaboratively, PFL methods aim to train a personalized model for each client. Most of existing PFL methods can be categorized as similarity-based methods [6], [9], [13], local customization-based methods [30], [32], [33], and meta-learning-based methods [34]–[36]. Similarity-based methods first compute the inter-client similarities and then perform the weighted federation of local models for each client based on these similarities. Specifically, clients with larger similarity scores are assigned larger weights for federated aggregation. In contrast, local customization-based methods, such as FedProx [30], incorporate a proximal term to customize personalized models for each client. Similarly, FedALA [37] captures the desired information from the global model in an element-wise manner and then aggregates the local models. As an alternative, FedPer [32] focuses on federating the backbone weights while training a personalized classification layer locally on each client. Additionally, meta-learning-based methods, such as [35], focus on discovering an initial

shared model that can be efficiently adapted to each client, enabling the creation of personalized local models. Due to the simplicity and effectiveness of similarity-based methods, we concentrate on similarity-based PFL methods in this paper. However, similarity-based PFL methods only consider the similarities between pairwise clients, while ignoring the critical complementarities between clients. Therefore, according to our theoretical findings, we propose to pursue not only similarities between different clients but also complementarities between different clients.

C. Spectral Graph Neural Networks

Spectral GNNs represent a class of GNNs that operate by designing graph signal filters in the spectral domain [18]. Specifically, they approximate filtering operations using polynomial bases of Laplacian eigenvalues [19]. For example, ChebNet [38] employs a K -order truncated Chebyshev polynomial basis to implement a K -hop localized filtering. However, Chien *et al.* [39] argue that the depth of ChebNet is limited in practice due to the over-smoothing phenomenon. To address this issue, they propose a Generalized PageRank (GPR) GNN (a.k.a. GPR-GNN [39]) that adaptively learns the GPR weights to control the contribution of each propagation step. However, the above-mentioned spectral GNNs learn the graph signal filters without a clear constraint, which may lead to oversimplified or ill-posed filters. To overcome this problem, BernNet [17] estimates the normalized Laplacian spectrum by a K -order Bernstein polynomial basis and learns the polynomial coefficients based on the observed graphs. Meanwhile, Wang *et al.* [18] theoretically analyze the expressive power of spectral GNNs and find the advantage of orthogonal polynomial bases. Inspired by their theoretical findings, they propose JacobiConv [18], which is based on the Jacobi polynomial basis due to its orthogonality and flexibility. Furthermore, OptBasisGNN [19] learns an orthogonal polynomial basis directly from the graph data. Nevertheless, the above-mentioned spectral GNNs can not deal with the varying homophily levels. To solve this problem, Huang *et al.* [40] propose the universal polynomial bases. Inspired by this work, we not only introduce the spectral GNN as the local model to tackle the issue of homophily heterogeneity across different clients, but also propose a novel federated aggregation method from the perspective of polynomial bases.

III. PRELIMINARIES

In this section, we introduce some mathematical notations related to the setting of GFL. In this paper, we concentrate on the task of node classification under the GFL scenario. In particular, we aim at the collaborative training of node classifiers with local subgraphs on different clients. Suppose we have M clients, each of which possesses a local subgraph $\mathcal{G}_m = \langle \mathcal{V}_m, \mathcal{E}_m \rangle$, where \mathcal{V}_m denotes the node set, \mathcal{E}_m represents the edge set, and $m = 1, \dots, M$. We utilize $\mathbf{X}_m \in \mathbb{R}^{n_m \times d}$ and $\mathbf{A}_m \in \mathbb{R}^{n_m \times n_m}$ to represent the node feature matrix and the adjacency matrix of \mathcal{G}_m , respectively. Here the number of nodes in \mathcal{G}_m and the feature dimension are denoted as n_m and d , respectively. Similarly, e_m and

c_m denote the number of edges and classes, respectively. In addition, let $\mathbf{L}_m = \mathbf{D}_m - \mathbf{A}_m = \mathbf{I} - \mathbf{D}_m^{-\frac{1}{2}} \mathbf{A}_m \mathbf{D}_m^{-\frac{1}{2}}$ denote the symmetric normalized Laplacian matrix of \mathcal{G}_m without self-loops, where \mathbf{D}_m is the degree matrix of \mathcal{G}_m , and \mathbf{I} is the identity matrix. Then, we can have the propagation matrix $\mathbf{P}_m = \mathbf{I} - \mathbf{L}_m$. Here we also introduce some norms used in this paper. First, we denote the l_2 -norm of a vector \mathbf{v} as $\|\mathbf{v}\|_2$, where $\|\mathbf{v}\|_2 = \sqrt{\sum_i v_i^2}$, and v_i is the i -th element of \mathbf{v} . Second, $\|\mathbf{X}\|_F$ denotes the Frobenius norm of a matrix \mathbf{X} , where $\|\mathbf{X}\|_F = \sqrt{\sum_{i,j} |x_{ij}|^2}$, and x_{ij} is the element of \mathbf{X} .

IV. THEORETICAL FOUNDATIONS

In this section, we theoretically analyze the heterogeneity in GFL and present our theoretical findings, which construct the theoretical foundation of our proposed method. First, we describe the construction of the federated collaboration graph, which is used to derive our theoretical findings. Second, we provide some definitions to facilitate the subsequent theorems. Third, we establish the relationship between the heterogeneity in GFL and the client's complementarity.

A. Federated Collaboration Graph

Inspired by pFedGraph [41], we construct a federated collaboration graph $\mathcal{G}_c = \langle \mathcal{V}_c, \mathcal{E}_c \rangle$ to model the collaboration strength between clients, where $\mathcal{V}_c = \{c_1, c_2, \dots, c_M\}$ represents the node set, \mathcal{E}_c is the edge set, and M is the number of clients. In \mathcal{G}_c , each node represents a client. Therefore, the adjacency matrix of \mathcal{G}_c is denoted as $\mathbf{W}_c \in \mathbb{R}^{M \times M}$, where \mathbf{W}_c^{ij} reflects the collaboration strength between the i -th and the j -th client. The neighbor set of node $u \in \mathcal{V}_c$ is denoted as \mathcal{N}_c . Here the degree of node u is denoted as $d_u = |\mathcal{N}_c|$. In addition, the degree matrix of \mathcal{G}_c is denoted as $\mathbf{D}_c \in \mathbb{R}^{M \times M}$, where $\mathbf{D}_c^{uu} = d_u$. Similarly, let $\mathbf{L}_c = \mathbf{D}_c - \mathbf{W}_c = \mathbf{I} - \mathbf{D}_c^{-\frac{1}{2}} \mathbf{W}_c \mathbf{D}_c^{-\frac{1}{2}}$ denote the symmetric normalized Laplacian matrix of \mathcal{G}_c without self-loops. We treat the model parameters on the i -th client (*i.e.*, θ_i) as the i -th node's features of \mathcal{G}_c . Therefore, the node feature matrix of \mathcal{G}_c can be represented as Θ , where $\Theta = [\theta_1, \theta_2, \dots, \theta_M]^T$, and $[\cdot, \cdot]$ denotes the concatenation operation. Consequently, the model aggregation of PFL (*i.e.*, weighted combination of model parameters among different clients) can be treated as the message passing of node features in \mathcal{G}_c .

B. Definitions

Here we first present some definitions to describe the similarities and complementarities between clients, respectively.

Definition 1. Similar Client Pair: Given any pair of clients i and j , the normalized similarity of their data distributions is defined as $S(i, j) \in [0, 1]$. If $S(i, j) \geq 0.5$, clients i and j are considered similar.

Definition 2. Complementary Client Pair: Given any pair of clients i and j , if $S(i, j) < 0.5$, clients i and j are considered complementary.

Definition 3. Similarity Ratio of Clients r_s : Given M clients performing federated learning, the similarity ratio of M clients r_s is the fraction of similar client pairs, *i.e.*,

$$r_s = \frac{|\{(i, j) \in \mathcal{E}_c : S(i, j) \geq 0.5\}|}{|\mathcal{E}_c|}. \quad (1)$$

Definition 4. Complementarity Ratio of Clients r_c : Given M clients performing federated learning, the complementarity ratio of M clients r_c is the fraction of complementary client pairs, *i.e.*,

$$r_c = \frac{|\{(i, j) \in \mathcal{E}_c : S(i, j) < 0.5\}|}{|\mathcal{E}_c|}. \quad (2)$$

Obviously, we can find that $r_c = 1 - r_s$. Based on the above definitions, we can find that a higher complementarity ratio means a higher level of heterophily.

To validate the practical meaning of the above definitions, we provide four examples on the *ogbn-arxiv* and *Amazon-ratings* datasets, respectively. As shown in Fig. 3, we plot the normalized similarity matrices under the non-overlapping and overlapping partitioning settings. According to our definition 3 and definition 4, we can easily obtain their similarity and complementarity ratios, respectively. The computed complementarity ratios are consistent with the practical situations. For example, the *Amazon-ratings* dataset has higher complementarity ratios than the *ogbn-arxiv* dataset, which is consistent with the observation that heterophilic datasets tend to have stronger heterophily than homophilic datasets [9]. Furthermore, since each five subgraphs are overlapped under the overlapping partitioning setting [6], datasets under the overlapping setting have smaller complementarity ratios than under the non-overlapping setting.

Second, we define the Laplacian frequency component from the spectral perspective.

Definition 5. Laplacian Frequency Component f : Consider the federated collaboration graph $\mathcal{G}_c = \langle \mathcal{V}_c, \mathcal{E}_c \rangle$ with the symmetric normalized Laplacian matrix \mathbf{L}_c . Given the node feature matrix Θ of \mathcal{G}_c , the Laplacian Frequency Component on \mathcal{G}_c is defined as $f(\Theta) = \text{Tr}(\frac{\Theta^T \mathbf{L}_c \Theta}{2})$, where “ $\text{Tr}(\cdot)$ ” computes the trace of the corresponding matrix.

Third, since the heterogeneity in GFL can be reflected in the Euclidean distance between any pair of client models [42]–[44], here we define a typical measure of heterogeneity in GFL as follows:

Definition 6. Measure of Heterogeneity in GFL $H(\mathcal{G}_c)$: Consider the federated collaboration graph \mathcal{G}_c with the adjacency matrix \mathbf{W}_c , the Measure of Heterogeneity $H(\mathcal{G}_c)$ is defined as $H(\mathcal{G}_c) = \sum_{(i,j) \in \mathcal{E}_c} \mathbf{W}_c^{ij} \|\theta_i - \theta_j\|_2^2$.

C. Relationship between Heterogeneity and Complementarity

Due to the characteristic of Laplacian matrix [19], the Laplacian frequency component $f(\Theta)$ actually captures the spectral frequency of the federated collaboration graph \mathcal{G}_c . Therefore, we present the following theorem (proved in the Appendix I-A) to formally describe the relationship between

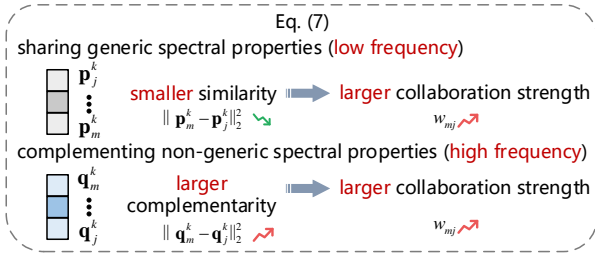


Fig. 5. To obtain the trade-off between sharing generic spectral properties and complementing non-generic spectral properties, an optimization problem with respect to the homophily bases and heterophily bases is formulated.

for its simplicity. Here, we use the UniFilter on the m -th client as an example to illustrate UniFilter's bases, including homophily bases and heterophily bases. First, based on the propagation matrix, the homophily bases \mathbf{H}_m can be defined as $\mathbf{H}_m = [\mathbf{H}_m^0, \mathbf{H}_m^1, \dots, \mathbf{H}_m^K]$, where $\mathbf{H}_m^K = \mathbf{P}_m^K \mathbf{X}_m$, $\mathbf{P}_m^K = (\mathbf{I} - \mathbf{L}_m)^K$, K is the order of homophily bases, and $[\cdot, \cdot]$ denotes the concatenation operation. Based on the definition of \mathbf{H}_m , we can find its physical meaning that the graph signal is propagated to K -hop neighbors via the propagation matrix \mathbf{P}_m . Therefore, this characteristic enables the homophily bases to effectively capture low-frequency information in the graph. Second, according to [40], the heterophily bases \mathbf{U}_m can be defined as $\mathbf{U}_m = [\mathbf{U}_m^0, \mathbf{U}_m^1, \dots, \mathbf{U}_m^K]$. Due to space limitations, details of the construction of heterophily bases are provided in the Appendix II. According to [40], the heterophily bases are prone to effectively capture high-frequency information in the graph. Given the constructed homophily and heterophily bases, the UniFilter can be defined as

$$\mathbf{Z}_m = \sum_{k=0}^K \mathbf{W}_m^k (\tau \mathbf{H}_m^k + (1 - \tau) \mathbf{U}_m^k), \quad (3)$$

where \mathbf{W}_m^k represents the learnable coefficients, $\tau \in [0, 1]$ is the hyperparameter adjusting the impact of homophily and heterophily bases, and \mathbf{Z}_m denotes the filtered spectral signal. Then, \mathbf{Z}_m is fed into a Multi-Layer Perceptron (MLP) to obtain the node classification results, namely

$$\hat{\mathbf{Y}}_m = \sigma(\mathbf{Z}_m \mathbf{W}_m^{\text{mlp}}), \quad (4)$$

where $\mathbf{W}_m^{\text{mlp}}$ represents the parameters of MLP, σ denotes the nonlinear activation function (*i.e.*, rectified linear unit (ReLU) [45] in our FedGSP), and $\hat{\mathbf{Y}}_m$ denotes the predicted results. Therefore, the learnable parameters on the m -th client consist of $\mathbf{W}_m^0, \mathbf{W}_m^1, \dots, \mathbf{W}_m^K$, and $\mathbf{W}_m^{\text{mlp}}$.

B. Optimization of the Collaboration Strengths

To obtain the trade-off between sharing generic spectral properties (*i.e.*, low-frequency information) and complementing non-generic spectral properties (*i.e.*, high-frequency information), we aim to formulate an optimization problem to determine the collaboration strengths (*i.e.*, \mathbf{W}_c) among clients. However, generic spectral properties (*i.e.*, low-frequency information) and non-generic spectral properties (*i.e.*, high-frequency information) can not be directly obtained. Fortunately, according to [40], low-frequency information and

high-frequency information are captured by the homophily bases and heterophily bases, respectively. Therefore, we can formulate a multi-objective optimization problem with respect to the homophily bases and heterophily bases, *i.e.*, pursuing the similarity of homophily bases while promoting the complementarity of heterophily bases. Fig. 5 is the schematic diagram to illustrate this optimization objective. However, due to privacy concerns, it is not allowed to upload the homophily and heterophily bases directly to the server. Therefore, inspired by [23], we design a pre-processing procedure to extract the principal components of the homophily and heterophily bases. Specifically, we first apply the Singular Value Decomposition (SVD) on the homophily and heterophily bases, respectively. For example, the SVD of \mathbf{H}_m^k and \mathbf{U}_m^k can be represented as

$$\mathbf{H}_m^k = \mathbf{Q}_m^{k,p} \Sigma_m^{k,p} (\mathbf{V}_m^{k,p})^T, \quad (5)$$

$$\mathbf{U}_m^k = \mathbf{Q}_m^{k,q} \Sigma_m^{k,q} (\mathbf{V}_m^{k,q})^T, \quad (6)$$

where $\mathbf{Q}_m^{k,p}$ and $\mathbf{Q}_m^{k,q}$ contain the singular vectors of \mathbf{H}_m^k and \mathbf{U}_m^k , respectively. Second, we select the first t columns of $\mathbf{Q}_m^{k,p}$ and $\mathbf{Q}_m^{k,q}$ and then flatten them to the vectors, denoted as \mathbf{p}_m^k and \mathbf{q}_m^k , respectively. By doing so, we not only eliminate the risk of data leakage but also greatly reduce the subsequent computation overhead.

Since each client has $K + 1$ homophily and heterophily bases, we can therefore construct $K + 1$ adjacency matrixes to separately determine the collaboration strength concerning the k -th order of bases ($k = 0, 1, \dots, K$). In other words, there are $K + 1$ optimization problems related to the bases (*i.e.*, optimizations of $\mathbf{W}_{c_0}, \mathbf{W}_{c_1}, \dots, \mathbf{W}_{c_K}$). We take the 0-th order of bases as the example to present the optimization process of \mathbf{W}_{c_0} . For ease of expression, here we abbreviate the \mathbf{W}_{c_0} , \mathbf{p}_m^0 , and \mathbf{q}_m^0 as \mathbf{W}_c , \mathbf{p}_m , and \mathbf{q}_m , respectively. Now we describe the objectives of our optimization problem, respectively. First, to pursue the similarity of homophily bases, a smaller Euclidean distance between homophily bases (*i.e.*, $\|\mathbf{p}_i - \mathbf{p}_j\|_2^2$) means a larger collaboration strength between the i -th and the j -th client (*i.e.*, w_{ij}). Second, to pursue the complementarity of heterophily bases, a larger Euclidean distance between heterophily bases (*i.e.*, $\|\mathbf{q}_i - \mathbf{q}_j\|_2^2$) means a larger collaboration strength between the i -th and the j -th client (*i.e.*, w_{ij}). Third, to adaptively adjust the importance of different dimensions of bases [46], we assign learnable self-attention weights (*i.e.*, \mathbf{R} and \mathbf{S}) to homophily and heterophily bases, respectively. In summary, the optimization objective can be written as

$$\begin{aligned} \min_{\mathbf{w}_c, \mathbf{R}, \mathbf{S}} \quad & \sum_{i=1}^M \sum_{j=1}^M (\|\mathbf{R}\mathbf{p}_i - \mathbf{R}\mathbf{p}_j\|_2^2 w_{ij} - \|\mathbf{S}\mathbf{q}_i - \mathbf{S}\mathbf{q}_j\|_2^2 w_{ij} \\ & + \gamma w_{ij}^2), \\ \text{s.t.} \quad & \forall i, \quad \mathbf{w}_i^\top \mathbf{1} = 1, \quad w_{ij} \geq 0, \\ & \mathbf{r}^\top \mathbf{1} = 1, r_l \geq 0, l = 1, 2, \dots, d \\ & \mathbf{s}^\top \mathbf{1} = 1, s_l \geq 0, l = 1, 2, \dots, d \\ & \mathbf{R} = \text{diag}(\mathbf{r}), \mathbf{S} = \text{diag}(\mathbf{s}), \end{aligned} \quad (7)$$

where $\mathbf{r} \in \mathbb{R}^d$ and $\mathbf{s} \in \mathbb{R}^d$ are learnable self-attention vectors, $\mathbf{R} \in \mathbb{R}^{d \times d}$ and $\mathbf{S} \in \mathbb{R}^{d \times d}$ are diagonal matrices,

$\mathbf{w}_i \in \mathbb{R}^{M \times 1}$ is the i -th column of \mathbf{W}_c , and w_{ij} is the element of \mathbf{W}_c . Inspired by [47], we employ a regularization term, i.e., γw_{ij}^2 , where γ is the regularization parameter. Without this regularization term, the optimization problem 7 would result in a trivial solution. Moreover, to further avoid the trivial solution, the sum of each column of \mathbf{W}_c is constrained to be 1 (i.e., $\mathbf{w}_i^\top \mathbf{1} = 1$, where $\mathbf{1}$ denotes the all-one column vector). Similarly, $\mathbf{r}^\top \mathbf{1} = 1$ and $\mathbf{s}^\top \mathbf{1} = 1$ are used to avoid trivial solutions of \mathbf{r} and \mathbf{s} , respectively. To solve the optimization objective in Eq. (7), inspired by [46], we update three variables (i.e., \mathbf{W}_c , \mathbf{R} , and \mathbf{S}) one by one in an iterative manner.

1) *Update \mathbf{R} with \mathbf{W}_c and \mathbf{S} Fixed:* Since \mathbf{W}_c and \mathbf{S} are fixed, the optimization objective in Eq. (7) can be written as

$$\begin{aligned} \min_{\mathbf{R}} \sum_{i=1}^M \sum_{j=1}^M \|\mathbf{R}\mathbf{p}_i - \mathbf{R}\mathbf{p}_j\|_2^2 w_{ij}, \\ \text{s.t. } \mathbf{r}^\top \mathbf{1} = 1, r_l \geq 0, l = 1, 2, \dots, d \\ \mathbf{R} = \text{diag}(\mathbf{r}). \end{aligned} \quad (8)$$

Here we introduce an elementary and very important theorem in spectral analysis [48], [49] to solve the above problem.

Theorem 4. *Given a matrix $\mathbf{O} \in \mathbb{R}^{M \times d}$, the i -th row of \mathbf{O} can be denoted as $\mathbf{o}_i^\top \in \mathbb{R}^{1 \times d}$. Consider the Laplacian matrix \mathcal{L}_c of the adjacency matrix \mathbf{W}_c , we can have*

$$2\text{Tr}(\mathbf{O}^\top \mathcal{L}_c \mathbf{O}) = \sum_{i=1}^M \sum_{j=1}^M \|\mathbf{o}_i - \mathbf{o}_j\|_2^2 \mathbf{W}_c^{ij}. \quad (9)$$

According to the theorem 4, we set the $\mathbf{o}_i = \mathbf{R}\mathbf{p}_i \in \mathbb{R}^{d \times 1} \Rightarrow \mathbf{O} = \mathbf{P}\mathbf{R}$. Therefore, Eq. (8) becomes

$$\begin{aligned} \min_{\mathbf{O}} \text{Tr}(\mathbf{O}^\top \mathcal{L}_c \mathbf{O}) \Rightarrow \min_{\mathbf{R}} \text{Tr}(\mathbf{R}\mathbf{P}^\top \mathcal{L}_c \mathbf{P}\mathbf{R}), \\ \text{s.t. } \mathbf{r}^\top \mathbf{1} = 1, r_l \geq 0, l = 1, 2, \dots, d \\ \mathbf{R} = \text{diag}(\mathbf{r}). \end{aligned} \quad (10)$$

Then, we employ the Lagrange multiplier method to solve the above problem. Due to space limitations, the detailed optimization process can be found in the Appendix III-A. Finally, we can have

$$r_i = \frac{1}{e_i^* \sum_{i=1}^d \frac{1}{e_i^*}}, \quad (11)$$

where $e_i^* = \mathbf{p}_{[:,i]}^\top \mathcal{L}_c \mathbf{p}_{[:,i]}$, $\mathbf{p}_{[:,i]} \in \mathbb{R}^{M \times 1}$ is the i -th column of \mathbf{P} , and $\mathbf{P} = [\mathbf{p}_1, \mathbf{p}_2, \dots, \mathbf{p}_M]^\top$.

2) *Update \mathbf{S} with \mathbf{W}_c and \mathbf{R} Fixed:* The update problem of \mathbf{S} when \mathbf{W}_c and \mathbf{R} are fixed is quite similar to the above problem in the Section V-B1. For simplicity, we leave the details in the Appendix III-B and directly give the result here. Specifically, we can have

$$s_i = \frac{1}{n_i^* \sum_{i=1}^d \frac{1}{n_i^*}}, \quad (12)$$

where $n_i^* = \mathbf{q}_{[:,i]}^\top \mathcal{L}_c \mathbf{q}_{[:,i]}$, $\mathbf{q}_{[:,i]} \in \mathbb{R}^{M \times 1}$ is the i -th column of \mathbf{Q} , and $\mathbf{Q} = [\mathbf{q}_1, \mathbf{q}_2, \dots, \mathbf{q}_M]^\top$.

3) *Update \mathbf{W}_c with \mathbf{S} and \mathbf{R} Fixed:* Since \mathbf{S} and \mathbf{R} are fixed, the optimization objective in Eq. (7) can be written as

$$\begin{aligned} \min_{\mathbf{W}_c} \sum_{i=1}^M \sum_{j=1}^M (\|\mathbf{R}\mathbf{p}_i - \mathbf{R}\mathbf{p}_j\|_2^2 w_{ij} - \|\mathbf{S}\mathbf{q}_i - \mathbf{S}\mathbf{q}_j\|_2^2 w_{ij} \\ + \gamma w_{ij}^2), \\ \text{s.t. } \forall i, \mathbf{w}_i^\top \mathbf{1} = 1, w_{ij} \geq 0. \end{aligned} \quad (13)$$

Since the optimization problem in Eq. (13) is independent across different clients for a specific client i , we can reformulate it as a subproblem tailored for the i -th client. Therefore, we can have

$$\begin{aligned} \min_{\mathbf{w}_i} \sum_{j=1}^M (\|\mathbf{R}\mathbf{p}_i - \mathbf{R}\mathbf{p}_j\|_2^2 w_{ij} - \|\mathbf{S}\mathbf{q}_i - \mathbf{S}\mathbf{q}_j\|_2^2 w_{ij} \\ + \gamma w_{ij}^2), \\ \text{s.t. } \mathbf{w}_i^\top \mathbf{1} = 1, w_{ij} \geq 0. \end{aligned} \quad (14)$$

Then, inspired by [46], we employ the Lagrange multiplier method and the Newton method to solve the above problem. Due to space limitations, the detailed optimization process can be found in the Appendix III-C. Finally, we can have

$$w_{ij}^* = (h_{ij} - \hat{b}_i^*)_+, \quad (15)$$

$$\hat{b}_i^* = \frac{1}{M} \sum_{j=1}^M (\hat{b}_i^* - h_{ij})_+, \quad (16)$$

where $h_{ij} = \frac{1}{M} - \frac{t_{ij}}{2\gamma} + \frac{\mathbf{1}^\top \mathbf{t}_i}{2M\gamma}$, $t_{ij} = \|\mathbf{R}\mathbf{p}_i - \mathbf{R}\mathbf{p}_j\|_2^2 - \|\mathbf{S}\mathbf{q}_i - \mathbf{S}\mathbf{q}_j\|_2^2$, and the optimal \hat{b}_i^* can be found by the Newton method.

C. Federated Aggregation for Polynomial Bases

Based on the optimized collaboration strengths, we can perform the federated aggregation. However, existing aggregation methods usually work on model weights or gradients, rarely on polynomial bases. Therefore, here we explore the aggregation method for polynomial bases. First, since polynomial bases are fundamental components in the spectral GNNs, we have to take into account their spectral properties when performing the federated aggregation. In Eq. (3), different orders of polynomial bases mean different propagation hops. For example, if $K = 3$, the graph signal is propagated to 3-hop neighbors. Therefore, we have to allow learnable coefficients \mathbf{W}_m^k to be federated separately according to each order k . Second, since polynomial bases may consist of information related to the graph data, we perform federated aggregation on coefficients instead of bases. Specifically, with the optimized collaboration strengths matrix \mathbf{W}_{c_k} corresponding to the k -th order of bases, we conduct the weighted averaging of coefficients across different clients. Our proposed separate federation can be defined as

$$\overline{\mathbf{W}}_m^k \leftarrow \sum_{j=1}^M w_{mj}^k \cdot \mathbf{W}_j^k, \quad (17)$$

where w_{mj}^k denotes the m, j -th element of \mathbf{W}_{c_k} and $\overline{\mathbf{W}}_m^k$ represents the aggregated coefficient.

Algorithm 1 FedGSP Client Algorithm

Input: Number of local epochs E ; the order of bases K ; number of selected columns t ; \mathcal{G}_m on client m ; node feature matrix \mathbf{X}_m on client m ; label matrix \mathbf{Y}_m on client m ; coefficients of bases $\mathbf{W}_m^{0:K}$ on client m ; parameters of MLP $\mathbf{W}_m^{\text{mlp}}$ on client m ; federated parameters $\overline{\mathbf{W}}_m^{\text{mlp}}$ and $\overline{\mathbf{W}}_m^{0:K}$ from the server.

Output: Predicted label $\hat{\mathbf{Y}}_m$.

- 1: Download federated parameters $\overline{\mathbf{W}}_m^{\text{mlp}}$ and $\overline{\mathbf{W}}_m^{0:K}$ from the server;
 - 2: $\mathbf{W}_m^{\text{mlp}} \leftarrow \overline{\mathbf{W}}_m^{\text{mlp}}$, $\mathbf{W}_m^{0:K} \leftarrow \overline{\mathbf{W}}_m^{0:K}$;
 - 3: Construct the homophily bases \mathbf{H}_m and heterophily bases \mathbf{U}_m for \mathcal{G}_m , respectively;
 - 4: **for** each local epoch e from 1 to E **do**
 - 5: Obtain the filtered spectral signal \mathbf{Z}_m via Eq. (3);
 - 6: Obtain the predicted results $\hat{\mathbf{Y}}_m$ via Eq. (4);
 - 7: Use cross-entropy loss to update $\mathbf{W}_m^{\text{mlp}}$ and $\mathbf{W}_m^{0:K}$;
 - 8: **for** k from 0 to K **do**
 - 9: Operate the SVD of \mathbf{H}_m and \mathbf{U}_m via Eq. (5) and Eq. (6) to obtain $\mathbf{Q}_m^{k,p}$ and $\mathbf{Q}_m^{k,q}$, respectively;
 - 10: Select the first t columns of $\mathbf{Q}_m^{k,p}$ and $\mathbf{Q}_m^{k,q}$ and then flatten them to obtain \mathbf{p}_m^k and \mathbf{q}_m^k , respectively;
 - 11: **end**
 - 12: **end**
 - 13: Upload $\mathbf{W}_m^{\text{mlp}}$, $\mathbf{W}_m^{0:K}$, $\mathbf{p}_m^{0:K}$, and $\mathbf{q}_m^{0:K}$ to the server.
-

Meanwhile, we consider the aggregation of $\mathbf{W}_m^{\text{mlp}}$. First, we have to obtain the collaboration strength matrix corresponding to the parameters of MLP (*i.e.*, \mathbf{W}_{cMLP}), which can be written as

$$\begin{aligned} \min_{\mathbf{W}_{\text{cMLP}}, \mathbf{R}_{\text{MLP}}, \mathbf{S}_{\text{MLP}}} & \sum_{i=1}^M \sum_{j=1}^M (\|\mathbf{R}_{\text{MLP}} \hat{\mathbf{p}}_i - \mathbf{R}_{\text{MLP}} \hat{\mathbf{p}}_j\|_2^2 w_{ij} \\ & - \|\mathbf{S}_{\text{MLP}} \hat{\mathbf{q}}_i - \mathbf{S}_{\text{MLP}} \hat{\mathbf{q}}_j\|_2^2 w_{ij} \\ & + \gamma w_{ij}^2), \\ \text{s.t. } & \forall i, \mathbf{w}_i^\top \mathbf{1} = 1, w_{ij} \geq 0, \\ & \mathbf{r}^\top \mathbf{1} = 1, r_l \geq 0, l = 1, 2, \dots, d \\ & \mathbf{s}^\top \mathbf{1} = 1, s_l \geq 0, l = 1, 2, \dots, d \\ & \mathbf{R}_{\text{MLP}} = \text{diag}(\mathbf{r}), \mathbf{S}_{\text{MLP}} = \text{diag}(\mathbf{s}), \end{aligned} \quad (18)$$

where $\hat{\mathbf{p}}_i = [\mathbf{p}_i^0, \mathbf{p}_i^1, \dots, \mathbf{p}_i^K]$, $\hat{\mathbf{p}}_j = [\mathbf{p}_j^0, \mathbf{p}_j^1, \dots, \mathbf{p}_j^K]$, $\hat{\mathbf{q}}_i = [\mathbf{q}_i^0, \mathbf{q}_i^1, \dots, \mathbf{q}_i^K]$, $\hat{\mathbf{q}}_j = [\mathbf{q}_j^0, \mathbf{q}_j^1, \dots, \mathbf{q}_j^K]$, $\mathbf{w}_i \in \mathbb{R}^{M \times 1}$ is the i -th column of \mathbf{W}_{cMLP} , $\mathbf{R}_{\text{MLP}} \in \mathbb{R}^{d \times d}$ and $\mathbf{S}_{\text{MLP}} \in \mathbb{R}^{d \times d}$ are self-attention matrices, and w_{ij} is the element of \mathbf{W}_{cMLP} . Then, the federation of $\mathbf{W}_m^{\text{mlp}}$ can be defined as

$$\overline{\mathbf{W}}_m^{\text{mlp}} \leftarrow \sum_{j=1}^M w_{mj}^{\text{mlp}} \cdot \mathbf{W}_j^{\text{mlp}}, \quad (19)$$

where w_{mj}^{mlp} denotes the m, j -th element of \mathbf{W}_{cMLP} , and $\overline{\mathbf{W}}_m^{\text{mlp}}$ represents the aggregated parameter. Eq. (19) can be similarly optimized by using the methods in the Section V-B. Finally, Algorithm 1 and Algorithm 2 summarize the main steps of our proposed FedGSP for the clients and the server, respectively.

Algorithm 2 FedGSP Server Algorithm

Input: Number of rounds R ; number of clients M ; the order of bases K ; coefficients of bases $\mathbf{W}_m^{0:K}$ from client m ; parameters of MLP $\mathbf{W}_m^{\text{mlp}}$ from client m ; pre-processed vectors $\mathbf{p}_m^{0:K}$ and $\mathbf{q}_m^{0:K}$ from client m .

Output: Federated parameters for clients.

- 1: Initialize parameters $(\overline{\mathbf{W}}^{\text{mlp}})^{(1)}$ and $(\overline{\mathbf{W}}^{0:K})^{(1)}$;
 - 2: **for** each round r from 1 to R **do**
 - 3: **for** client $m \in \{1, 2, \dots, M\}$ **in parallel do**
 - 4: **if** $r = 1$ **then**
 - 5: Send $(\overline{\mathbf{W}}^{\text{mlp}})^{(r)}$ and $(\overline{\mathbf{W}}^{0:K})^{(r)}$ to client m ;
 - 6: **end**
 - 7: **else**
 - 8: Receive $\mathbf{W}_m^{\text{mlp}}$ and $\mathbf{W}_m^{0:K}$ from client m ;
 - 9: Receive $\mathbf{p}_m^{0:K}$ and $\mathbf{q}_m^{0:K}$ from client m ;
 - 10: **for** k from 0 to K **do**
 - 11: Optimize \mathbf{W}_{ck} via Eq. (7) to Eq. (16);
 - 12: **end**
 - 13: Obtain $(\overline{\mathbf{W}}_m^{0:K})^{(r)}$ via Eq. (17);
 - 14: Optimize \mathbf{W}_{cMLP} by solving Eq. (18);
 - 15: Obtain $(\overline{\mathbf{W}}_m^{\text{mlp}})^{(r)}$ via Eq. (19);
 - 16: Send $(\overline{\mathbf{W}}_m^{\text{mlp}})^{(r)}$ and $(\overline{\mathbf{W}}_m^{0:K})^{(r)}$ to client m ;
 - 17: **end**
 - 18: Perform Algorithm 1 on client m ;
 - 19: **end**
 - 20: **end**
-

D. Efficiency Analysis

Here we present the spatial and temporal complexities of different methods on the client and server sides in Tab. I, respectively. Due to space limitations, the detailed efficiency analysis of our proposed FedGSP is provided in the Appendix IV. According to Tab. I, we can find that the temporal complexity of our proposed FedGSP is mainly related to the optimization process (*i.e.*, $\mathcal{O}(M \times d \times (M + d + 1))$), which is independent of the local model training. Therefore, in the practical implementation, we implement the optimization process and the local model training in parallel, so that our proposed FedGSP is efficient in real-world applications, which is also validated by our experiments (see Section VI-F).

VI. EXPERIMENTS

To demonstrate the effectiveness of our proposed **F**ederated learning method by mining **G**raph **S**pectral **P**roperties (FedGSP), intensive experiments are carried out on eleven well-known graph datasets, including six homophilic datasets and five heterophilic datasets. In particular, we perform experiments on a large-scale graph dataset (*i.e.*, *ogbn-arxiv*), which consists of more than millions of edges. First, we compare our proposed FedGSP with eleven state-of-the-art methods under both the non-overlapping and overlapping subgraph partitioning settings. Second, we conduct ablation studies to evaluate the effectiveness of sharing generic spectral properties and complementing non-generic spectral properties, respectively. Third, we perform case studies to analyze the spectral properties captured by the local model after federation. Fourth,

TABLE I

THE SPATIAL AND TEMPORAL COMPLEXITIES OF DIFFERENT METHODS ON THE CLIENT AND SERVER SIDES, RESPECTIVELY. HERE M , K , d , n_m , e_m , AND c_m DENOTE THE NUMBER OF CLIENTS, ORDERS, DIMENSIONS, NODES, EDGES, AND CLASSES, RESPECTIVELY.

Method	Client Spa. Comp.	Server Spa. Comp.	Client Temp. Comp.	Server Temp. Comp.
FedAvg [25]	$\mathcal{O}(d + d^2)$	$\mathcal{O}(M \times (1 + d^2))$	$\mathcal{O}(e_m \times d + n_m \times d^2)$	$\mathcal{O}(M)$
FedProx [30]	$\mathcal{O}(d + 2d^2)$	$\mathcal{O}(M \times (1 + d^2))$	$\mathcal{O}(e_m \times d + n_m \times d^2 + d^2)$	$\mathcal{O}(M)$
FedPer [32]	$\mathcal{O}(d + 2d^2)$	$\mathcal{O}(M \times (1 + d^2))$	$\mathcal{O}(e_m \times d + n_m \times d^2 + d^2)$	$\mathcal{O}(M)$
GCFL [50]	$\mathcal{O}(d + d^2)$	$\mathcal{O}(M \times (1 + 2d^2))$	$\mathcal{O}(e_m \times d + n_m \times d^2)$	$\mathcal{O}(M + M^2 \times (\log M + d^2))$
FedGNN [51]	$\mathcal{O}(d + 2d^2)$	$\mathcal{O}(2M \times (1 + 2d^2))$	$\mathcal{O}(e_m \times d + n_m \times d^2 + d)$	$\mathcal{O}(M)$
FedSage+ [26]	$\mathcal{O}(n_m \times d + 3d^2)$	$\mathcal{O}(M \times (1 + 3d^2))$	$\mathcal{O}(e_m \times d + n_m \times d^2)$	$\mathcal{O}(M)$
FED-PUB [6]	$\mathcal{O}(n_m \times d + d^2)$	$\mathcal{O}(M \times (d^2 + M))$	$\mathcal{O}(e_m \times d + n_m \times d^2)$	$\mathcal{O}(M \times d \times (M + d))$
FedGTA [13]	$\mathcal{O}(d + d^2 + K \times c_m)$	$\mathcal{O}(M \times (1 + d^2 + M \times K \times c_m))$	$\mathcal{O}(e_m \times (d + n_m \times c_m) + n_m \times (d^2 + c_m))$	$\mathcal{O}(M + M \times K \times c_m)$
AdaFGL [28]	$\mathcal{O}(n_m \times d + 2d^2)$	$\mathcal{O}(M \times (1 + d^2))$	$\mathcal{O}(K \times (e_m \times d + e_m \times n_m + n_m \times d^2))$	$\mathcal{O}(M)$
FedTAD [8]	$\mathcal{O}(n_m \times d + 2d^2)$	$\mathcal{O}(M \times (1 + d^2))$	$\mathcal{O}(K \times n_m + e_m)$	$\mathcal{O}(n_m \times d \times (d + n_m + 2M \times c_m))$
FedIIH [9]	$\mathcal{O}(n_m \times d + d^2)$	$\mathcal{O}(M \times K \times (d^2 + M))$	$\mathcal{O}(K \times (e_m \times d + n_m \times d^2))$	$\mathcal{O}(M \times d \times (K \times M + d))$
FedGSP (Ours)	$\mathcal{O}(K \times d + d^2)$	$\mathcal{O}(M \times K \times (d^2 + M))$	$\mathcal{O}(K \times (e_m \times d + n_m \times d^2))$	$\mathcal{O}(M \times d \times (M + d + 1) + M \times K)$

we plot the convergence curves of our proposed FedGSP and the baseline methods. In addition, to reveal the advantage of our proposed FedGSP over the baseline methods in terms of efficiency, we report the communication round time of the proposed FedGSP and the compared baseline methods. Furthermore, we perform a detailed sensitivity analysis on the hyperparameters used in our proposed FedGSP. The implementation details are presented in the Appendix V.

A. Experimental Settings

In our experiments, eleven state-of-the-art methods are employed for comparison. Concretely, we adopt one classic Federated Learning (FL) method (*i.e.*, FedAvg [25]), two personalized FL methods (*i.e.*, FedProx [30] and FedPer [32]), three general GFL methods (*i.e.*, GCFL [50], FedGNN [51], and FedSage+ [26]), and five personalized GFL methods (*i.e.*, FED-PUB [6], FedGTA [13], AdaFGL [28], FedTAD [8], and FedIIH [9]). To ensure the fairness of experiments, according to [6], [9], all methods are repeated three times, where the mean accuracies and standard deviations are both reported.

B. Experimental Results

Our proposed FedGSP is compared with the above-mentioned baseline methods on both homophilic and heterophilic datasets.

1) *Homophilic Datasets*: Tab. II and Tab. III show the comparison results on the homophilic datasets in two partitioning settings, respectively. Our proposed FedGSP achieves the best performance among most of the baseline methods. Moreover, the standard deviations of FedGSP are relatively small, indicating that FedGSP is more stable than the compared baseline methods. Although the average accuracies of FedGSP for all six datasets in both non-overlapping and overlapping scenarios are only slightly higher than the second-best method (*i.e.*, FedIIH [9]), our proposed FedGSP is more efficient than FedIIH (see the Section VI-F), achieving more than three times speed improvement. Since some conventional baseline methods can not well deal with the heterogeneity, they have large standard deviations. For example, the standard deviations of FedAvg, FedProx, and FedSage+ are 5.64, 4.56, and 5.94 on the *Cora* datasets with 5 clients, respectively. Although some recent methods alleviate the node feature heterogeneity and structure heterogeneity to some extent, FedGSP still performs

better than them. This is because FedGSP not only shares generic spectral properties but also complements non-generic spectral properties, so that it effectively learns graphs with varying homophily levels across different clients.

2) *Heterophilic Datasets*: Tab. IV and Tab. V show the comparison results on the heterophilic datasets in two partitioning settings, respectively. Our proposed FedGSP not only obtains the best performance among most of the baseline methods, but also outperforms the second-best method (*i.e.*, FedIIH [9]) by an average margin of 3.28% and 1.61% in the non-overlapping and overlapping scenarios, respectively. Furthermore, since the heterogeneity of heterophilic graph datasets is generally stronger than that of the homophilic graph datasets [9], [28], heterophilic graph datasets are usually more challenging than homophilic graph datasets. However, our proposed FedGSP still outperforms the second-best method (*i.e.*, FedIIH) in both kinds of graph datasets and achieves a larger performance gain on the heterophilic datasets than on the homophilic datasets, which validates the effectiveness of mining graph spectral properties.

C. Ablation Study

Since our proposed FedGSP not only shares generic spectral properties but also complements non-generic spectral properties, we carry out the ablation experiments to shed light on the contributions of these two strategies. Specifically, we employ the ‘Sharing’ and ‘Complementing’ to represent sharing generic spectral properties and complementing non-generic spectral properties, respectively. Depending on whether these two strategies are used, there are a total of four combinations, as shown in Tab. VI. We can clearly observe that the performance decreases when any strategy is removed, indicating that each strategy contributes a lot to the final performance. For example, the accuracies on the *Cora* dataset are obviously reduced when both two strategies are removed.

D. Case Study

Since our proposed FedGSP not only shares generic spectral properties but also complements non-generic spectral properties among different clients, one might wonder what spectral properties are captured by local models after federation. Therefore, we carry out the case studies to analyze the spectral properties captured by local models after the federated

TABLE II

ACCURACY COMPARISON OF VARIOUS METHODS ON SIX **HOMOPHILIC** GRAPH DATASETS IN THE **NON-OVERLAPPING** SUBGRAPH PARTITIONING SETTING. THE BEST AND SECOND-BEST RECORDS ON EACH DATASET ARE HIGHLIGHTED IN **BOLD** AND UNDERLINED, RESPECTIVELY.

Methods	Cora			CiteSeer			PubMed			
	5 Clients	10 Clients	20 Clients	5 Clients	10 Clients	20 Clients	5 Clients	10 Clients	20 Clients	
Local	81.30±0.21	79.94±0.24	80.30±0.25	69.02±0.05	67.82±0.13	65.98±0.17	84.04±0.18	82.81±0.39	82.65±0.03	
FedAvg [25]	74.45±5.64	69.19±0.67	69.50±3.58	71.06±0.60	63.61±3.59	64.68±1.83	79.40±0.11	82.71±0.29	80.97±0.26	
FedProx [30]	72.03±4.56	60.18±7.04	48.22±6.18	71.73±1.11	63.33±3.25	64.85±1.35	79.45±0.25	82.55±0.24	80.50±0.25	
FedPer [32]	81.68±0.40	79.35±0.04	78.01±0.32	70.41±0.32	70.53±0.28	66.64±0.27	85.80±0.21	84.20±0.28	84.72±0.31	
GCFL [50]	81.47±0.65	78.66±0.27	79.21±0.70	70.34±0.57	69.01±0.12	66.33±0.05	85.14±0.33	84.18±0.19	83.94±0.36	
FedGNN [51]	81.51±0.68	70.12±0.99	70.10±3.52	69.06±0.92	55.52±3.17	52.23±6.00	79.52±0.23	83.25±0.45	81.61±0.59	
FedSage+ [26]	72.97±5.94	69.05±1.59	57.97±12.6	70.74±0.69	65.63±3.10	65.46±0.74	79.57±0.24	82.62±0.31	80.82±0.25	
FED-PUB [6]	83.70±0.19	81.54±0.12	81.75±0.56	72.68±0.44	72.35±0.53	67.62±0.12	86.79±0.09	86.28±0.18	85.53±0.30	
FedGTA [13]	80.06±0.63	80.59±0.38	79.01±0.31	70.12±0.10	71.57±0.34	69.94±0.14	87.75±0.01	86.80±0.01	87.12±0.05	
AdaFGL [28]	82.01±0.51	80.09±0.00	79.74±0.05	71.44±0.27	72.34±0.00	70.95±0.45	86.91±0.28	86.97±0.10	86.99±0.21	
FedTAD [8]	80.31±0.26	80.87±0.11	80.07±0.15	70.34±0.37	69.43±0.75	68.09±0.69	84.00±0.13	84.61±0.17	84.33±0.18	
FedIIIH [9]	84.11±0.17	81.85±0.09	83.01±0.15	72.86±0.25	76.50±0.06	73.36±0.41	87.80±0.18	87.65±0.18	87.19±0.25	
FedGSP (Ours)	84.72±0.06	83.00±0.10	83.66±0.08	73.60±0.11	77.35±0.09	72.28±0.33	88.20±0.09	87.89±0.13	87.52±0.10	
Methods	Amazon-Computer			Amazon-Photo			ogbn-arxiv			Avg.
	5 Clients	10 Clients	20 Clients	5 Clients	10 Clients	20 Clients	5 Clients	10 Clients	20 Clients	All
Local	89.22±0.13	88.91±0.17	89.52±0.20	91.67±0.09	91.80±0.02	90.47±0.15	66.76±0.07	64.92±0.09	65.06±0.05	79.57
FedAvg [25]	84.88±1.96	79.54±0.23	74.79±0.24	89.89±0.83	83.15±3.71	81.35±1.04	65.54±0.07	64.44±0.10	63.24±0.13	74.58
FedProx [30]	85.25±1.27	83.81±1.09	73.05±1.30	90.38±0.48	80.92±4.64	82.32±0.29	65.21±0.20	64.37±0.18	63.03±0.04	72.84
FedPer [32]	89.67±0.34	89.73±0.04	87.86±0.43	91.44±0.37	91.76±0.23	90.59±0.06	66.87±0.05	64.99±0.18	64.66±0.11	79.94
GCFL [50]	89.07±0.91	90.03±0.16	89.08±0.25	91.99±0.29	92.06±0.25	90.79±0.17	66.80±0.12	65.09±0.08	65.08±0.04	79.90
FedGNN [51]	88.08±0.15	88.18±0.41	83.16±0.13	90.25±0.70	87.12±2.01	81.00±4.48	65.47±0.22	64.21±0.32	63.80±0.05	75.23
FedSage+ [26]	85.04±0.61	80.50±1.13	70.42±0.85	90.77±0.44	76.81±8.24	80.58±1.15	65.69±0.09	64.52±0.14	63.31±0.20	73.47
FED-PUB [6]	90.74±0.05	90.55±0.13	90.12±0.09	93.29±0.19	92.73±0.18	91.92±0.12	67.77±0.09	66.58±0.08	66.64±0.12	81.59
FedGTA [13]	86.69±0.18	86.66±0.23	85.01±0.87	93.33±0.12	93.50±0.21	92.61±0.15	60.32±0.04	60.22±0.09	59.74±0.14	79.45
AdaFGL [28]	80.20±0.05	83.62±0.26	84.53±0.23	86.69±0.19	89.85±0.83	88.11±0.05	52.73±0.19	51.77±0.36	50.94±0.08	76.97
FedTAD [8]	82.20±1.20	85.50±0.33	83.91±1.54	92.29±0.39	90.59±0.09	89.18±0.84	65.35±0.14	64.06±0.25	64.45±0.13	78.87
FedIIIH [9]	90.74±0.13	90.86±0.23	90.44±0.05	93.42±0.02	94.22±0.08	93.55±0.09	70.30±0.06	69.34±0.02	68.65±0.04	83.10
FedGSP (Ours)	91.08±0.09	91.08±0.12	90.38±0.06	93.63±0.04	94.28±0.10	93.72±0.07	70.57±0.06	69.40±0.01	68.72±0.09	83.39

TABLE III

ACCURACY COMPARISON OF VARIOUS METHODS ON SIX **HOMOPHILIC** GRAPH DATASETS IN THE **OVERLAPPING** SUBGRAPH PARTITIONING SETTING. THE BEST AND SECOND-BEST RECORDS ON EACH DATASET ARE HIGHLIGHTED IN **BOLD** AND UNDERLINED, RESPECTIVELY.

Methods	Cora			CiteSeer			PubMed			
	10 Clients	30 Clients	50 Clients	10 Clients	30 Clients	50 Clients	10 Clients	30 Clients	50 Clients	
Local	73.98±0.25	71.65±0.12	76.63±0.10	65.12±0.08	64.54±0.42	66.68±0.44	82.32±0.07	80.72±0.16	80.54±0.11	
FedAvg [25]	76.48±0.36	53.99±0.98	53.99±4.53	69.48±0.15	66.15±0.64	66.51±1.00	82.67±0.11	82.05±0.12	80.24±0.35	
FedProx [30]	77.85±0.50	51.38±1.74	56.27±9.04	69.39±0.35	66.11±0.75	66.53±0.43	82.63±0.17	82.13±0.13	80.50±0.46	
FedPer [32]	78.73±0.31	74.18±0.24	74.42±0.37	69.81±0.28	65.19±0.81	67.64±0.44	85.31±0.06	84.35±0.38	83.94±0.10	
GCFL [50]	78.84±0.26	73.41±0.27	76.63±0.16	69.48±0.39	64.92±0.18	65.98±0.30	83.59±0.25	80.77±0.12	81.36±0.11	
FedGNN [51]	70.63±0.83	61.38±2.33	56.91±0.82	68.72±0.39	59.98±1.52	58.98±0.98	84.25±0.07	82.02±0.22	81.85±0.10	
FedSage+ [26]	77.52±0.46	51.99±0.42	55.48±11.5	68.75±0.48	65.97±0.02	65.93±0.30	82.77±0.08	82.14±0.11	80.31±0.68	
FED-PUB [6]	79.60±0.12	75.40±0.54	77.84±0.23	70.58±0.20	68.33±0.45	69.21±0.30	85.70±0.08	85.16±0.10	84.84±0.12	
FedGTA [13]	76.42±0.62	75.63±0.33	77.69±0.14	70.43±0.08	71.71±0.33	69.19±0.32	85.34±0.42	84.99±0.05	84.47±0.06	
AdaFGL [28]	78.50±0.19	75.80±0.23	74.41±0.00	72.63±0.15	68.18±0.31	62.90±0.75	85.58±0.23	85.85±0.41	84.45±0.07	
FedTAD [8]	79.29±0.78	60.92±2.17	68.08±0.44	73.47±0.16	67.74±0.57	63.51±0.68	82.98±0.20	82.11±0.15	81.63±0.19	
FedIIIH [9]	80.57±0.23	76.82±0.24	78.58±0.25	73.16±0.18	72.27±0.21	69.56±0.11	85.87±0.03	86.65±0.11	85.65±0.12	
FedGSP (Ours)	80.99±0.15	76.86±0.12	77.82±0.09	72.28±0.05	72.55±0.13	69.79±0.13	87.21±0.06	86.92±0.15	85.31±0.15	
Methods	Amazon-Computer			Amazon-Photo			ogbn-arxiv			Avg.
	10 Clients	30 Clients	50 Clients	10 Clients	30 Clients	50 Clients	10 Clients	30 Clients	50 Clients	All
Local	88.50±0.20	86.66±0.00	87.04±0.02	92.17±0.12	90.16±0.12	90.42±0.15	62.52±0.07	61.32±0.04	60.04±0.04	76.72
FedAvg [25]	88.99±0.19	83.37±0.47	76.34±0.12	92.91±0.07	89.30±0.22	74.19±0.57	63.56±0.02	59.72±0.06	60.94±0.24	73.38
FedProx [30]	88.84±0.20	83.84±0.89	76.60±0.47	92.67±0.19	89.17±0.40	72.36±2.06	63.52±0.11	59.86±0.16	61.12±0.04	73.38
FedPer [32]	89.30±0.04	87.99±0.23	88.22±0.27	92.88±0.24	91.23±0.16	90.92±0.38	63.97±0.08	62.29±0.04	61.24±0.11	78.42
GCFL [50]	89.01±0.22	87.24±0.09	87.02±0.22	92.45±0.10	90.58±0.11	90.54±0.08	63.24±0.02	61.66±0.10	60.32±0.01	77.61
FedGNN [51]	88.15±0.09	87.00±0.10	83.96±0.88	91.47±0.11	87.91±1.34	78.90±6.46	63.08±0.19	60.09±0.04	60.51±0.11	73.66
FedSage+ [26]	89.24±0.15	81.33±1.20	76.72±0.39	92.76±0.05	88.69±0.99	72.41±1.36	63.24±0.02	59.90±0.12	60.95±0.09	73.12
FED-PUB [6]	89.98±0.08	89.15±0.06	88.76±0.14	93.22±0.07	92.01±0.07	91.71±0.11	64.18±0.04	63.34±0.12	62.55±0.12	79.53
FedGTA [13]	90.10±0.18	88.79±0.27	88.15±0.21	93.13±0.14	92.49±0.06	91.77±0.06	55.98±0.09	56.76±0.07	57.89±0.09	74.40
AdaFGL [28]	80.49±0.00	80.42±0.00	82.12±0.00	89.24±0.00	88.34±0.00	87.68±0.00	56.81±0.06	55.17±0.00	54.82±0.00	75.74
FedTAD [8]	79.09±5.63	79.48±0.85	77.05±0.07	81.94±3.09	86.58±1.75	84.38±1.33	58.45±0.15	57.75±0.54	56.52±0.14	73.39
FedIIIH [9]	90.15±0.04	89.56±0.19	89.99±0.00	93.38±0.00	94.17±0.04	93.25±0.16	66.69±0.09	66.10±0.03	66.67±0.06	81.01
FedGSP (Ours)	90.27±0.06	89.67±0.11	89.31±0.00	93.69±0.03	94.33±0.05	93.28±0.07	67.34±0.04	66.18±0.02	65.64±0.08	81.08

TABLE IV

COMPARISON OF VARIOUS METHODS ON FIVE **HETEROPHILIC** GRAPH DATASETS IN THE **NON-OVERLAPPING** SUBGRAPH PARTITIONING SETTING. ACCURACY (%) IS REPORTED FOR *Roman-empire* AND *Amazon-ratings*, AND AUC (%) IS REPORTED FOR *Minesweeper*, *Tolokers*, AND *Questions*. THE BEST AND SECOND-BEST RECORDS ON EACH DATASET ARE HIGHLIGHTED IN **BOLD** AND UNDERLINED, RESPECTIVELY.

Methods	Roman-empire			Amazon-ratings			Minesweeper		
	5 Clients	10 Clients	20 Clients	5 Clients	10 Clients	20 Clients	5 Clients	10 Clients	20 Clients
Local	33.65±0.13	28.42±0.26	23.89±0.32	45.03±0.31	45.89±0.19	46.02±0.02	71.35±0.17	69.96±0.16	69.31±0.09
FedAvg [25]	38.93±0.32	35.43±0.32	32.00±0.39	41.26±0.53	41.66±0.14	42.20±0.21	72.60±0.08	71.84±0.02	71.36±0.16
FedProx [30]	27.95±0.59	26.43±1.41	23.12±0.49	36.92±0.00	36.86±0.14	36.96±0.05	71.91±0.27	70.66±0.20	71.50±0.37
FedPer [32]	20.75±1.75	15.51±1.13	15.45±2.76	36.62±0.30	32.34±1.01	36.96±0.03	58.73±10.45	65.35±7.02	53.80±11.40
GCFL [50]	30.40±0.16	29.44±0.49	26.73±0.19	36.92±0.00	36.86±0.14	36.96±0.02	72.04±0.13	71.14±0.09	47.77±0.14
FedGNN [51]	30.26±0.11	29.09±0.01	26.60±0.02	36.80±0.06	36.72±0.00	36.45±0.09	72.55±0.13	71.08±0.07	71.71±0.27
FedSage+ [26]	57.26±0.00	49.07±0.00	38.36±0.00	36.82±0.00	36.71±0.00	37.03±0.02	77.74±0.00	72.80±0.00	69.70±0.00
FED-PUB [6]	40.80±0.26	36.77±0.30	32.67±0.39	44.41±0.41	44.85±0.17	45.39±0.50	72.18±0.02	71.56±0.05	70.72±0.40
FedGTA [13]	61.56±0.27	60.94±0.19	59.65±0.28	41.22±0.66	39.40±0.44	39.24±0.12	45.60±1.41	64.97±0.35	49.63±8.64
AdaFGL [28]	67.64±0.18	64.55±0.00	62.42±0.26	41.70±0.06	42.30±0.00	42.59±0.14	47.45±2.10	65.59±0.56	51.48±7.14
FedTAD [8]	45.26±0.19	44.71±0.38	42.04±0.13	43.59±0.33	43.35±0.29	44.50±0.26	69.52±0.06	70.74±0.09	72.74±0.03
FedIIIH [9]	68.32±0.05	66.44±0.28	64.61±0.13	44.26±0.24	44.24±0.10	45.19±0.04	74.29±0.02	73.23±0.04	72.81±0.02
FedGSP (Ours)	68.80±0.04								

TABLE V

COMPARISON OF VARIOUS METHODS ON FIVE HETEROPHILIC GRAPH DATASETS IN THE OVERLAPPING SUBGRAPH PARTITIONING SETTING. ACCURACY (%) IS REPORTED FOR *Roman-empire* AND *Amazon-ratings*, AND AUC (%) IS REPORTED FOR *Minesweeper*, *Tolokers*, AND *Questions*. THE BEST AND SECOND-BEST RECORDS ON EACH DATASET ARE HIGHLIGHTED IN BOLD AND UNDERLINED, RESPECTIVELY.

Methods	Roman-empire			Amazon-ratings			Minesweeper			-
	10 Clients	30 Clients	50 Clients	10 Clients	30 Clients	50 Clients	10 Clients	30 Clients	50 Clients	-
Local	39.47±0.03	34.43±0.14	31.28±0.18	41.43±0.04	41.81±0.14	42.57±0.12	67.98±0.07	64.39±0.10	62.73±0.23	-
FedAvg [25]	40.89±0.25	38.66±0.08	36.71±0.20	39.86±0.06	41.40±0.02	41.02±0.16	69.06±0.07	67.95±0.04	66.89±0.08	-
FedPer [30]	36.63±0.14	35.31±0.17	33.61±0.59	37.00±0.00	36.60±0.00	36.89±0.00	68.27±0.05	66.75±0.19	66.03±0.16	-
FedPer [32]	23.66±3.27	23.27±3.09	22.23±3.58	32.33±4.23	31.58±0.54	34.48±2.25	61.85±1.02	60.13±1.38	60.06±3.61	-
GCFL [50]	37.65±0.27	36.32±0.19	34.80±0.09	37.00±0.00	36.60±0.00	36.89±0.00	68.47±0.06	67.13±0.10	67.41±12.56	-
FedGNN [51]	37.46±0.12	36.47±0.24	34.92±0.26	36.58±0.16	36.77±0.12	36.95±0.15	68.59±0.21	67.30±0.17	66.41±0.23	-
FedSage+ [26]	57.48±0.00	42.55±0.00	33.99±0.00	36.86±0.00	36.71±0.00	37.03±0.00	76.64±0.00	70.56±0.00	70.34±0.00	-
FED-PUB [6]	43.80±0.25	40.46±0.16	37.73±0.09	42.25±0.25	42.25±0.06	42.88±0.34	68.80±0.09	67.43±0.25	65.98±0.15	-
FedGTA [13]	59.86±0.04	58.32±0.09	57.57±0.21	40.81±0.24	39.44±0.06	39.37±0.04	54.35±0.73	48.20±1.28	52.94±1.77	-
AdaFGL [28]	64.44±0.03	61.77±0.02	59.55±0.01	39.39±0.05	41.19±0.15	40.71±0.25	55.15±0.84	50.15±1.63	54.18±2.15	-
FedTAD [8]	44.14±0.13	41.94±0.18	40.82±0.01	39.53±0.17	40.69±0.13	40.58±0.26	68.69±0.08	68.43±0.05	66.66±0.05	-
FedIII [9]	65.48±0.12	63.32±0.06	62.42±0.10	42.63±0.02	42.40±0.05	42.65±0.21	69.35±0.25	68.09±0.26	67.37±0.14	-
FedGSP (Ours)	65.81±0.13	63.96±0.19	62.92±0.07	42.79±0.04	42.60±0.06	42.98±0.12	75.70±0.17	75.08±0.15	71.52±0.09	-
Methods	Tolokers			Questions			Avg.			-
	10 Clients	30 Clients	50 Clients	10 Clients	30 Clients	50 Clients	10 Clients	30 Clients	50 Clients	All
Local	73.83±0.03	69.01±0.31	66.63±0.20	63.17±0.02	57.17±0.08	56.13±0.02	57.18	53.36	51.87	54.14
FedAvg [25]	72.99±0.40	58.51±0.27	55.47±0.42	62.80±0.63	58.88±0.18	60.78±0.27	57.12	53.08	52.17	54.12
FedPer [30]	54.49±1.69	45.59±0.41	41.49±0.45	52.53±0.34	51.54±0.41	50.72±0.40	49.78	47.16	45.75	47.56
FedPer [32]	39.60±1.11	59.44±0.79	41.92±0.06	61.31±0.29	53.41±1.53	50.29±0.10	43.75	45.57	41.80	43.70
GCFL [50]	55.91±1.13	47.91±0.59	18.40±0.25	53.04±0.47	51.84±0.38	51.10±0.38	50.41	43.03	39.72	44.39
FedGNN [51]	56.21±1.20	46.85±0.31	42.18±0.45	53.25±0.15	51.90±0.15	51.22±0.14	50.42	47.86	46.34	48.97
FedSage+ [26]	74.54±0.00	70.88±0.00	69.61±0.00	64.22±0.00	65.34±0.00	62.76±0.00	61.95	57.21	54.75	57.97
FED-PUB [6]	74.17±0.29	70.35±0.54	66.80±0.85	65.39±2.44	58.38±1.19	58.76±0.16	58.88	55.77	54.43	56.36
FedGTA [13]	40.02±1.70	47.34±0.75	45.81±1.96	35.56±5.46	50.43±1.05	53.33±0.40	46.12	48.75	49.80	48.22
AdaFGL [28]	45.15±2.15	49.18±0.84	47.54±2.48	41.05±6.49	52.18±2.16	56.46±0.92	49.04	50.89	51.69	50.54
FedTAD [8]	69.27±1.26	62.11±0.27	56.39±0.52	59.28±0.28	59.24±0.36	57.81±0.24	56.18	54.48	52.45	54.37
FedIII [9]	71.67±0.02	71.69±0.12	69.99±0.03	68.79±0.09	66.98±0.04	64.73±0.35	63.58	62.50	61.43	62.50
FedGSP (Ours)	74.41±0.03	72.21±0.12	70.52±0.09	69.38±0.07	66.27±0.03	65.54±0.14	65.62	64.02	62.70	64.11

TABLE VI

ABLATION STUDIES IN BOTH NON-OVERLAPPING AND OVERLAPPING PARTITIONING SETTINGS ON THE *Cora* AND *Roman-empire* DATASETS.

		Cora					
Sharing	Complementing	non-overlapping 5 clients	non-overlapping 10 clients	non-overlapping 20 clients	overlapping 10 clients	overlapping 30 clients	overlapping 50 clients
✓	✗	82.52±0.21 (↓ 2.20)	80.26±0.15 (↓ 2.74)	81.55±0.22 (↓ 2.11)	78.84±0.21 (↓ 2.15)	74.51±0.14 (↓ 2.35)	75.76±0.16 (↓ 2.06)
✗	✓	71.52±0.43 (↓ 13.20)	74.14±0.21 (↓ 8.86)	78.32±0.16 (↓ 5.34)	77.32±0.19 (↓ 3.67)	73.98±0.33 (↓ 2.88)	75.00±0.22 (↓ 2.82)
✗	✗	64.61±0.34 (↓ 20.11)	76.38±0.23 (↓ 6.62)	77.30±0.18 (↓ 6.36)	78.32±0.35 (↓ 2.67)	74.72±0.31 (↓ 2.14)	71.49±0.18 (↓ 6.33)
✓	✓	84.72±0.06	83.00±0.10	83.66±0.08	80.99±0.15	76.86±0.12	77.82±0.09
		Roman-empire					
Sharing	Complementing	non-overlapping 5 clients	non-overlapping 10 clients	non-overlapping 20 clients	overlapping 10 clients	overlapping 30 clients	overlapping 50 clients
✓	✗	65.40±0.18 (↓ 3.40)	65.57±0.16 (↓ 2.15)	62.70±0.12 (↓ 2.72)	62.84±0.17 (↓ 2.97)	62.33±0.24 (↓ 1.63)	60.89±0.16 (↓ 2.03)
✗	✓	58.69±0.41 (↓ 10.11)	65.46±0.18 (↓ 2.26)	63.14±0.18 (↓ 2.28)	62.27±0.15 (↓ 3.54)	61.00±0.21 (↓ 2.96)	60.30±0.15 (↓ 2.62)
✗	✗	56.30±0.15 (↓ 12.50)	63.11±0.17 (↓ 4.61)	61.03±0.14 (↓ 4.39)	63.06±0.18 (↓ 2.75)	61.02±0.26 (↓ 2.94)	60.64±0.14 (↓ 2.28)
✓	✓	68.80±0.04	67.72±0.09	65.42±0.07	65.81±0.13	63.96±0.19	62.92±0.07

aggregation. Comparing Fig. 2 and Fig. 6, we can find that our proposed FedGSP allows the local model on each client not only to preserve its local graph spectral properties, but also to obtain the additional spectral properties from collaborations. For example, compared with Fig. 2a and Fig. 2b, Fig. 6a and Fig. 6b show both the low-frequency and high-frequency properties due to obtaining the additional spectral properties from collaborations. Similarly, compared with Fig. 2d, the low-frequency properties are strengthened in Fig. 6d. Furthermore, compared with Fig. 2c, the low-frequency properties are strengthened in Fig. 6c due to preserving its local graph spectral properties.

E. Convergence Curves

Here we plot the convergence curves of our proposed FedGSP and the baseline methods in Fig. 7 and Fig. 8. We can find that our proposed FedGSP converges fastly within several communication rounds (e.g., Fig. 7b and Fig. 8h). Moreover, the fluctuations in the curves of our FedGSP are quite low, which confirms its stability. These results validate that FedGSP can be employed for various practical applications. This can be attributed to our efficient optimization method. In contrast, the convergence curves of GCFL (e.g., Fig. 7h) and FedGTA (e.g., Fig. 8a) are not stable enough. This is because GCFL and FedGTA perform the federated aggregation based on the

clustering result and the similarity matrix between clients, respectively. However, both are unstable across communication rounds due to variations in local models caused by homophily heterogeneity.

F. Time of Each Communication Round

To demonstrate the efficiency of our proposed FedGSP over the baseline methods, we report the time of each communication round for the proposed FedGSP and the compared baseline methods. According to Tab. VII, the time cost of our proposed method is significantly lower than the average in most scenarios. Furthermore, we can find that our proposed FedGSP is more efficient than several promising baseline methods (i.e., FED-PUB and FedIII). Specifically, compared to the second-best baseline method (i.e., FedIII), FedGSP achieves more than three times speed improvement. For example, on the *Cora* dataset in the overlapping subgraph partitioning setting with 30 clients, the accuracies of FedGSP and FedIII are 76.86 and 76.82, respectively. However, the time cost of our FedGSP and FedIII are 7.30 seconds and 65.49 seconds, respectively. This is because, in each communication round, FedIII employs a hierarchical variation inference model to infer the distribution of the subgraph data on each client, which is computationally expensive. Although our proposed FedGSP utilizes the Lagrange multiplier method

TABLE VII
THE TIME (SECONDS) OF EACH COMMUNICATION ROUND FOR THE PROPOSED FEDGSP AND THE COMPARED BASELINE METHODS ON THE *Cora* AND *Roman-empire* DATASETS.

Cora						
Methods	non-overlapping 5 clients	non-overlapping 10 clients	non-overlapping 20 clients	overlapping 10 clients	overlapping 30 clients	overlapping 50 clients
FedAvg [25]	5.51	2.19	5.63	5.40	7.27	12.08
FedProx [30]	4.24	4.65	8.86	5.49	13.71	22.43
FedPer [32]	4.06	4.13	8.17	4.16	12.38	20.24
GCFL [50]	6.44	9.42	18.63	9.04	27.70	46.77
FedGNN [51]	2.28	4.42	8.76	5.40	13.07	23.04
FedSage+ [26]	6.88	8.55	17.88	9.37	16.97	23.35
FED-PUB [6]	22.04	27.34	60.31	33.46	80.54	147.84
FedGTA [13]	3.36	2.24	5.89	4.30	5.00	7.18
AdaFGL [28]	1.99	2.49	4.63	4.44	6.16	7.83
FedTAD [8]	4.91	5.25	9.13	5.22	12.84	19.71
FedIIIH [9]	19.57	22.76	56.09	19.67	65.49	139.03
FedGSP (Ours)	6.73	2.26	5.86	5.18	7.30	11.90
Average	7.33	7.98	17.49	9.26	22.37	40.12
Roman-empire						
Methods	non-overlapping 5 clients	non-overlapping 10 clients	non-overlapping 20 clients	overlapping 10 clients	overlapping 30 clients	overlapping 50 clients
FedAvg [25]	8.20	5.76	8.46	10.25	18.47	19.12
FedProx [30]	4.31	6.73	9.04	6.90	16.25	23.66
FedPer [32]	5.35	6.19	9.19	6.47	15.58	20.22
GCFL [50]	6.58	9.39	18.32	10.78	29.05	50.58
FedGNN [51]	3.33	6.60	9.43	6.45	15.29	22.82
FedSage+ [26]	10.06	14.82	26.27	23.09	47.42	62.72
FED-PUB [6]	18.81	28.03	61.75	28.45	83.07	133.05
FedGTA [13]	2.17	3.58	5.32	3.42	6.12	9.92
AdaFGL [28]	4.34	4.14	5.55	6.49	7.80	10.69
FedTAD [8]	4.88	8.55	15.03	10.98	22.42	37.01
FedIIIH [9]	17.45	24.90	47.01	28.19	61.17	100.10
FedGSP (Ours)	9.09	5.80	8.70	10.39	18.36	19.13
Average	7.88	10.37	18.67	12.66	28.42	42.42

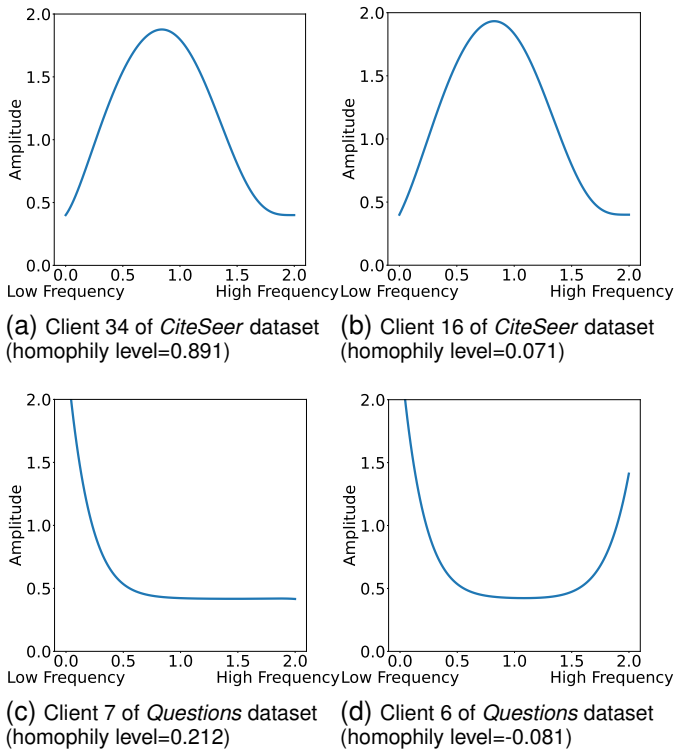


Fig. 6. Spectral properties captured by local models after the federated aggregation.

and the Newton method to optimize the collaboration graphs, their time complexity is small. Although several baseline methods (*i.e.*, AdaFGL and FedGNN) cost less time than our FedGSP, their performances are not good enough than FedGSP. In addition, the time cost of FedGSP slowly increases as the number of clients increases, demonstrating that our

proposed FedGSP is acceptable in real-world applications.

G. Sensitivity Analysis on Hyperparameters

Here we perform a detailed sensitivity analysis on the hyperparameters used in our proposed FedGSP. There are four hyperparameters (*i.e.*, number of orders K , number of selected columns t , regularization parameter γ , and τ) in our FedGSP. First, we plot the accuracy curves along with the variance bar under different values of K and t , respectively. As shown in Fig. 9, the variations in performance under different values of K and t are both small. Second, as shown in Fig. 10, the variations in performance under different values of γ and τ are both small. These experimental results clearly demonstrate that the performances of FedGSP are very stable within a given range of hyperparameters. In other words, the hyperparameters of our proposed FedGSP can be easily tuned for practical use.

VII. CONCLUSION

In this paper, we propose a novel **F**ederated learning method by mining **G**raph **S**pectral **P**roperties (FedGSP), which effectively mines graph spectral properties to learn graphs with varying homophily levels across different clients. On one hand, FedGSP enables clients to share generic spectral properties, and thus all clients can benefit through collaboration. On the other hand, it allows clients to complement non-generic spectral properties to obtain additional information gain. To the best of our knowledge, this is the *first* time in GFL that alleviates the homophily heterogeneity. Therefore, our method achieves promising performances on eleven datasets and outperforms the second-best method by an average margin of 3.28% on all heterophilic graph datasets.

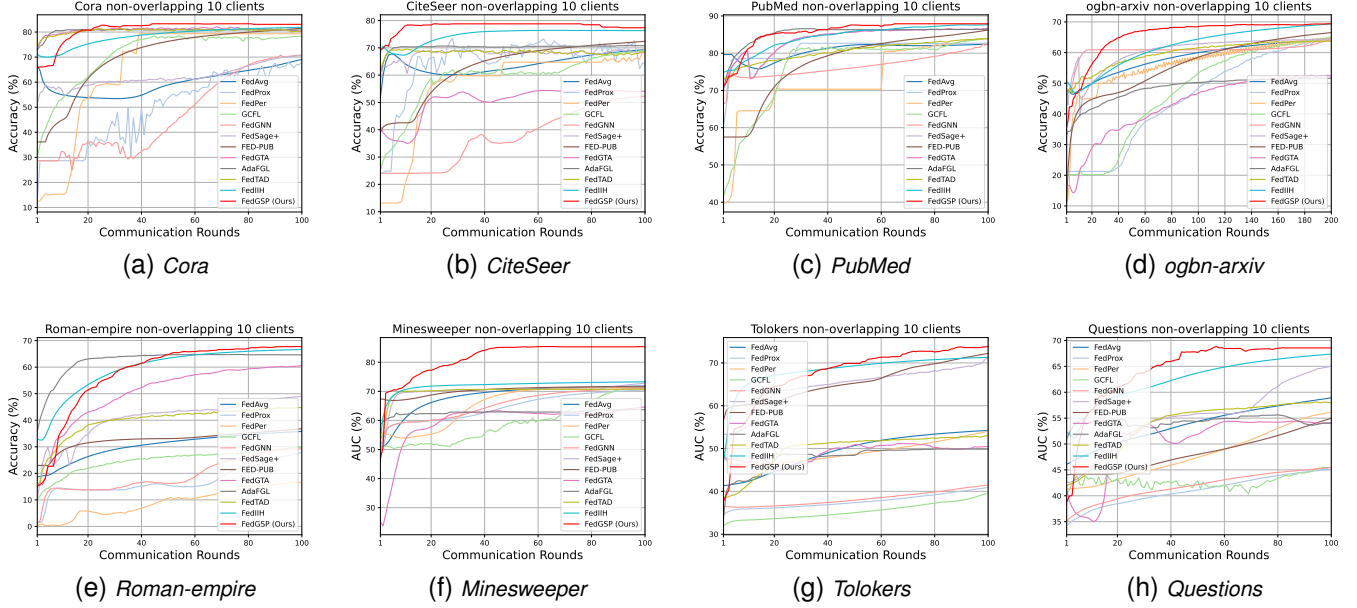


Fig. 7. Convergence curves in the non-overlapping partitioning settings on eight datasets with 10 clients.

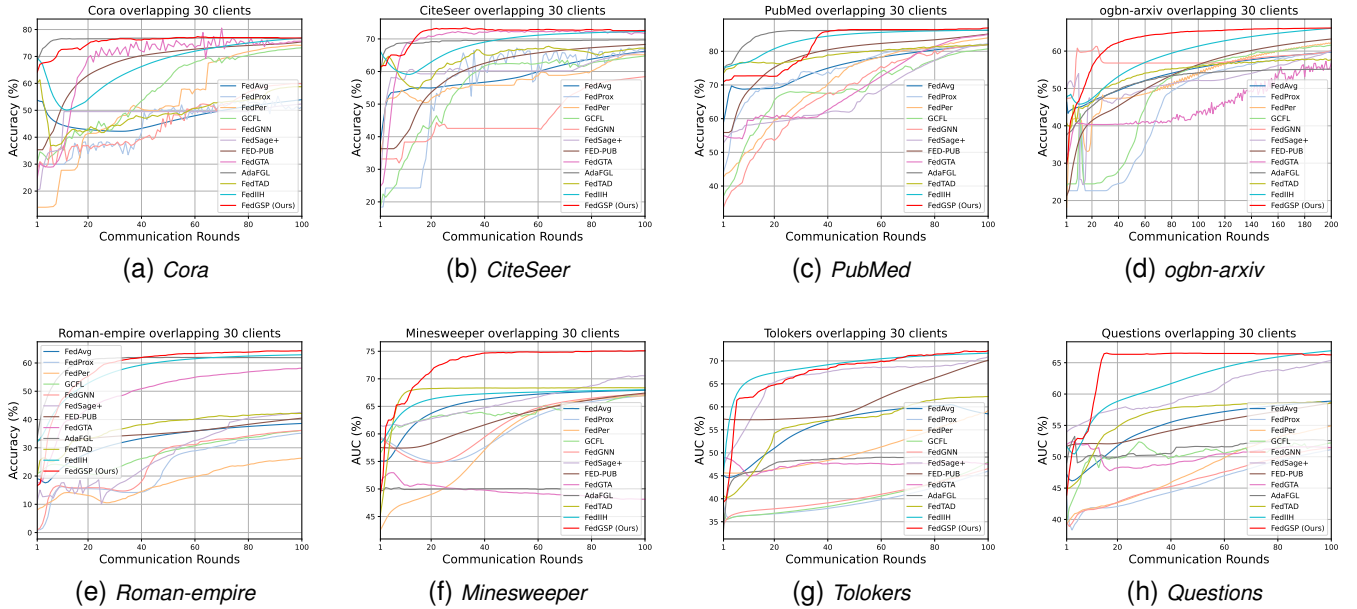


Fig. 8. Convergence curves in the overlapping partitioning settings on eight datasets with 30 clients.

REFERENCES

[1] M. Guang, C. Yan, Y. Xu, J. Wang, and C. Jiang, “Graph convolutional networks with adaptive neighborhood awareness,” *IEEE Transactions on Pattern Analysis and Machine Intelligence*, vol. 46, no. 11, pp. 7392–7404, 2024.

[2] K. Zhang, Q. Wen, C. Zhang, R. Cai, M. Jin, Y. Liu, J. Y. Zhang, Y. Liang, G. Pang, D. Song, and S. Pan, “Self-supervised learning for time series analysis: Taxonomy, progress, and prospects,” *IEEE Transactions on Pattern Analysis and Machine Intelligence*, vol. 46, no. 10, pp. 6775–6794, 2024.

[3] W. Yu, S. Chen, C. Gong, G. Niu, and M. Sugiyama, “Atom-motif contrastive transformer for molecular property prediction,” *arXiv preprint arXiv:2310.07351*, 2023.

[4] W. Yu, S. Wan, G. Li, J. Yang, and C. Gong, “Hyperspectral image classification with contrastive graph convolutional network,” *IEEE Transactions on Geoscience and Remote Sensing*, vol. 61, no. 1, pp. 1–15, 2023.

[5] J. Bai, W. Yu, Z. Xiao, V. Havyarimana, A. C. Regan, H. Jiang, and L. Jiao, “Two-stream spatial-temporal graph convolutional networks for driver drowsiness detection,” *IEEE Transactions on Cybernetics*, vol. 52, no. 12, pp. 13 821–13 833, 2022.

[6] J. Baek, W. Jeong, J. Jin, J. Yoon, and S. J. Hwang, “Personalized subgraph federated learning,” in *International Conference on Machine Learning*, 2023, pp. 1396–1415.

[7] W. Huang, G. Wan, M. Ye, and B. Du, “Federated graph semantic and structural learning,” in *International Joint Conference on Artificial Intelligence*, 2023, pp. 1–9.

[8] Y. Zhu, X. Li, Z. Wu, D. Wu, M. Hu, and R.-H. Li, “FedTAD: Topology-aware data-free knowledge distillation for subgraph federated learning,” in *International Joint Conference on Artificial Intelligence*, 2024, pp. 1–9.

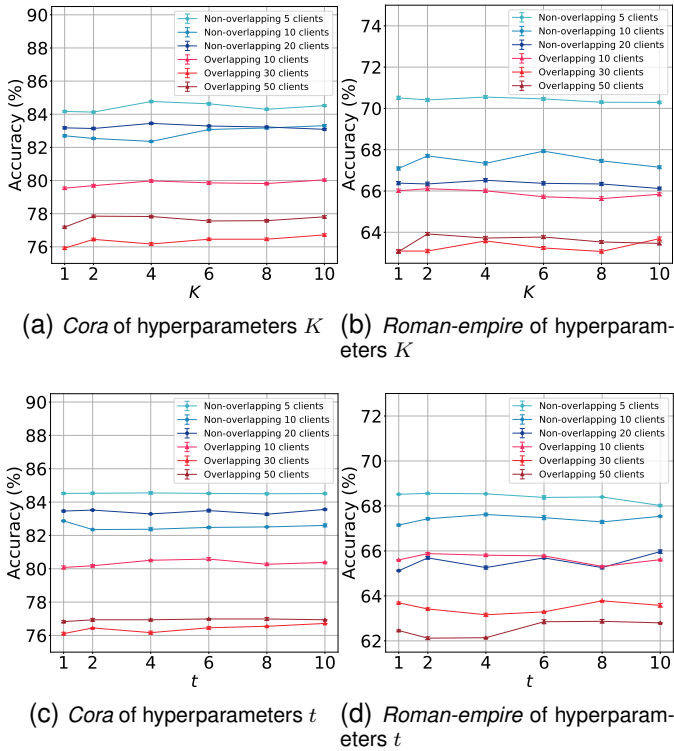


Fig. 9. The sensitivity analyses of hyperparameters K and t , respectively.

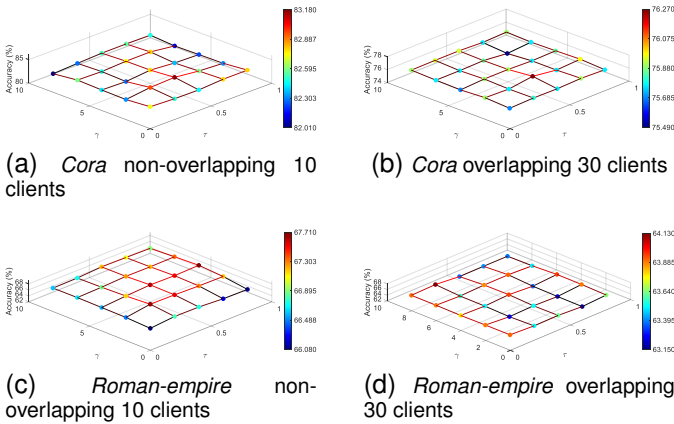


Fig. 10. The sensitivity analyses of hyperparameters γ and τ .

[9] W. Yu, S. Chen, Y. Tong, T. Gu, and C. Gong, “Modeling inter-intra heterogeneity for graph federated learning,” in *AAAI Conference on Artificial Intelligence*, 2025, pp. 1–9.

[10] W. Huang, M. Ye, Z. Shi, G. Wan, H. Li, B. Du, and Q. Yang, “Federated learning for generalization, robustness, fairness: A survey and benchmark,” *IEEE Transactions on Pattern Analysis and Machine Intelligence*, vol. 46, no. 12, pp. 9387–9406, 2024.

[11] W. Huang, M. Ye, Z. Shi, and B. Du, “Generalizable heterogeneous federated cross-correlation and instance similarity learning,” *IEEE Transactions on Pattern Analysis and Machine Intelligence*, vol. 46, no. 2, pp. 712–728, 2024.

[12] Y. Zhao, Q. Liu, P. Liu, X. Liu, and K. He, “Medical federated model with mixture of personalized and shared components,” *IEEE Transactions on Pattern Analysis and Machine Intelligence*, vol. 47, no. 1, pp. 433–449, 2025.

[13] X. Li, Z. Wu, W. Zhang, Y. Zhu, R.-H. Li, and G. Wang, “FedGTA: Topology-aware averaging for federated graph learning,” in *International Conference on Very Large Databases*, 2023, pp. 41–50.

[14] O. Platonov, D. Kuznedelev, A. Babenko, and L. Prokhorenkova, “Characterizing graph datasets for node classification: Homophily-heterophily dichotomy and beyond,” in *Advances in Neural Information Processing Systems*, 2023, pp. 523–548.

[15] J. Zhu, Y. Yan, L. Zhao, M. Heimann, L. Akoglu, and D. Koutra, “Beyond homophily in graph neural networks: Current limitations and effective designs,” in *Advances in Neural Information Processing Systems*, 2020, pp. 7793–7804.

[16] M. Balcilar, G. Renton, P. Héroux, B. Gaüzère, S. Adam, and P. Honeine, “Analyzing the expressive power of graph neural networks in a spectral perspective,” in *International Conference on Learning Representations*, 2021, pp. 1–26.

[17] M. He, Z. Wei, Z. Huang, and H. Xu, “Bernnet: Learning arbitrary graph spectral filters via bernstein approximation,” in *Advances in Neural Information Processing Systems*, 2021, pp. 14 239–14 251.

[18] X. Wang and M. Zhang, “How powerful are spectral graph neural networks,” in *International Conference on Machine Learning*, 2022, pp. 23 341–23 362.

[19] Y. Guo and Z. Wei, “Graph neural networks with learnable and optimal polynomial bases,” in *International Conference on Machine Learning*, 2023, pp. 12 077–12 097.

[20] Z. Tan, G. Wan, W. Huang, and M. Ye, “FedSSP: Federated graph learning with spectral knowledge and personalized preference,” in *Advances in Neural Information Processing Systems*, 2024, pp. 1–15.

[21] H. Zhou, W. Yu, S. Wan, Y. Tong, T. Gu, and C. Gong, “Traffic pattern sharing for federated traffic flow prediction with personalization,” in *International Conference on Data Mining*, 2024, pp. 1–10.

[22] J. Chen, R. Lei, and Z. Wei, “PolyGCL: Graph contrastive learning via learnable spectral polynomial filters,” in *International Conference on Learning Representations*, 2024, pp. 1–30.

[23] K. Yan, S. Cui, A. Wuerkaixi, J. Zhang, B. Han, G. Niu, M. Sugiyama, and C. Zhang, “Balancing similarity and complementarity for federated learning,” in *International Conference on Machine Learning*, 2024, pp. 1–18.

[24] T. N. Kipf and M. Welling, “Semi-supervised classification with graph convolutional networks,” in *International Conference on Learning Representations*, 2017, pp. 1–14.

[25] B. McMahan, E. Moore, D. Ramage, S. Hampson, and B. A. y Arcas, “Communication-efficient learning of deep networks from decentralized data,” in *International Conference on Artificial Intelligence and Statistics*, 2017, pp. 1273–1282.

[26] K. Zhang, C. Yang, X. Li, L. Sun, and S. M. Yiu, “Subgraph federated learning with missing neighbor generation,” in *Advances in Neural Information Processing Systems*, 2021, pp. 6671–6682.

[27] W. Hamilton, Z. Ying, and J. Leskovec, “Inductive representation learning on large graphs,” in *Advances in Neural Information Processing Systems*, 2017, pp. 1–11.

[28] X. Li, Z. Wu, W. Zhang, H. Sun, R.-H. Li, and G. Wang, “AdaFGL: A new paradigm for federated node classification with topology heterogeneity,” in *International Conference on Data Engineering*, 2024, pp. 2517–2530.

[29] M. Ye, X. Fang, B. Du, P. C. Yuen, and D. Tao, “Heterogeneous federated learning: State-of-the-art and research challenges,” *ACM Computing Surveys*, vol. 56, no. 3, pp. 1–44, 2023.

[30] T. Li, A. K. Sahu, M. Zaheer, M. Sanjabi, A. Talwalkar, and V. Smith, “Federated optimization in heterogeneous networks,” in *Annual Conference on Machine Learning and Systems*, 2020, pp. 429–450.

[31] A. Z. Tan, H. Yu, L. Cui, and Q. Yang, “Towards personalized federated learning,” *IEEE Transactions on Neural Networks and Learning Systems*, vol. 34, no. 12, pp. 9587–9603, 2023.

[32] M. G. Arivazhagan, V. Aggarwal, A. K. Singh, and S. Choudhary, “Federated learning with personalization layers,” *arXiv:1912.00818*, 2019. [Online]. Available: <https://arxiv.org/abs/1912.00818>

[33] C. T. Dinh, N. Tran, and J. Nguyen, “Personalized federated learning with moreau envelopes,” in *Advances in Neural Information Processing Systems*, 2020, pp. 21 394–21 405.

[34] F. Chen, M. Luo, Z. Dong, Z. Li, and X. He, “Federated meta-learning with fast convergence and efficient communication,” *arXiv:1802.07876*, 2018. [Online]. Available: <https://arxiv.org/abs/1802.07876>

[35] A. Fallah, A. Mokhtari, and A. Ozdaglar, “Personalized federated learning with theoretical guarantees: A model-agnostic meta-learning approach,” in *Advances in Neural Information Processing Systems*, 2020, pp. 3557–3568.

[36] E. Baccour, A. Erbad, A. Mohamed, M. Hamdi, and M. Guizani, “A blockchain-based reliable federated meta-learning for metaverse: A dual game framework,” *IEEE Internet of Things Journal*, pp. 22 697–22 715, 2024.

- [37] J. Zhang, Y. Hua, H. Wang, T. Song, Z. Xue, R. Ma, and H. Guan, "FedALA: Adaptive local aggregation for personalized federated learning," in *AAAI Conference on Artificial Intelligence*, 2023, pp. 1–8.
- [38] M. Defferrard, X. Bresson, and P. Vandergheynst, "Convolutional neural networks on graphs with fast localized spectral filtering," in *Advances in Neural Information Processing Systems*, 2016, pp. 1–9.
- [39] E. Chien, J. Peng, P. Li, and O. Milenkovic, "Adaptive universal generalized pagerank graph neural network," in *International Conference on Learning Representations*, 2021, pp. 1–24.
- [40] K. Huang, Y. G. Wang, M. Li, and P. Lio, "How universal polynomial bases enhance spectral graph neural networks: Heterophily, over-smoothing, and over-squashing," in *International Conference on Machine Learning*, 2024, pp. 1–20.
- [41] R. Ye, Z. Ni, F. Wu, S. Chen, and Y. Wang, "Personalized federated learning with inferred collaboration graphs," in *International Conference on Machine Learning*, 2023, pp. 39 801–39 817.
- [42] M. Luo, F. Chen, D. Hu, Y. Zhang, J. Liang, and J. Feng, "No fear of heterogeneity: Classifier calibration for federated learning with non-iid data," in *Advances in Neural Information Processing Systems*, 2021, pp. 5972–5984.
- [43] S. Vahidian, M. Morafah, C. Chen, M. Shah, and B. Lin, "Rethinking data heterogeneity in federated learning: Introducing a new notion and standard benchmarks," *IEEE Transactions on Artificial Intelligence*, vol. 5, no. 3, pp. 1386–1397, 2023.
- [44] R. Ye, Z. Ni, C. Xu, J. Wang, S. Chen, and Y. C. Eldar, "FedFM: Anchor-based feature matching for data heterogeneity in federated learning," *IEEE Transactions on Signal Processing*, vol. 71, no. 1, pp. 4224–4239, 2023.
- [45] V. Nair and G. E. Hinton, "Rectified linear units improve restricted boltzmann machines," in *International Conference on Machine Learning*, 2010, pp. 807–814.
- [46] F. Nie, D. Wu, R. Wang, and X. Li, "Self-weighted clustering with adaptive neighbors," *IEEE Transactions on Neural Networks and Learning Systems*, vol. 31, no. 9, pp. 3428–3441, 2020.
- [47] F. Nie, X. Wang, and H. Huang, "Clustering and projected clustering with adaptive neighbors," in *ACM SIGKDD International Conference on Knowledge Discovery and Data Mining*, 2014, pp. 977–986.
- [48] F. Nie, G. Cai, J. Li, and X. Li, "Auto-weighted multi-view learning for image clustering and semi-supervised classification," *IEEE Transactions on Image Processing*, vol. 27, no. 3, pp. 1501–1511, 2018.
- [49] Y. Luo, B. Han, and C. Gong, "A bi-level formulation for label noise learning with spectral cluster discovery," in *International Joint Conference on Artificial Intelligence*, 2020, pp. 2605–2611.
- [50] H. Xie, J. Ma, L. Xiong, and C. Yang, "Federated graph classification over non-iid graphs," in *Advances in Neural Information Processing Systems*, 2021, pp. 18 839–18 852.
- [51] C. Wu, F. Wu, Y. Cao, Y. Huang, and X. Xie, "FedGNN: Federated graph neural network for privacy-preserving recommendation," *arXiv:2102.04925*, 2021. [Online]. Available: <https://arxiv.org/abs/2102.04925>